

Late Pleistocene and Holocene paleoenvironmental reconstruction of a drowned karst isolation basin (Lošinj Channel, NE Adriatic Sea)

Brunović, Dea; Miko, Slobodan; Hasan, Ozren; Papatheodorou, George; Ilijanić, Nikolina; Misericchi, Stefano; Correggiari, Annamaria; Geraga, Maria

Source / Izvornik: **Palaeogeography, Palaeoclimatology, Palaeoecology, 2020, 544**

Journal article, Accepted version

Rad u časopisu, Završna verzija rukopisa prihvaćena za objavljivanje (postprint)

<https://doi.org/10.1016/j.palaeo.2020.109587>

Permanent link / Trajna poveznica: <https://um.nsk.hr/um:nbn:hr:245:201427>

Rights / Prava: [In copyright](#)/[Zaštićeno autorskim pravom.](#)

Download date / Datum preuzimanja: **2025-03-09**



Repository / Repozitorij:

[Repository of the Croatian Geological Survey](#)



1 **Late Pleistocene and Holocene paleoenvironmental reconstruction of a drowned karst isolation**
2 **basin (Lošinj Channel, NE Adriatic Sea)**

3 Dea Brunović^{a*}, Slobodan Miko^a, Ozren Hasan^a, George Papatheodorou^b, Nikolina Ilijanić^a, Stefano
4 Miserocchi^c, Annamaria Correggiari^c, Maria Geraga^b

5 ^aCroatian Geological Survey, Sachsova 2, 10000 Zagreb, Croatia

6 ^bLaboratory of Marine Geology and Physical Oceanography, Department of Geology, University of
7 Patras, 26504, Greece

8 ^cInstituto di Scienze Marine (ISMAR-CNR), Via Gobetti 101, 40129 Bologna, Italy

9 * Corresponding Author: Dea Brunović, E-mail: dea.brunovic@hgi-cgs.hr

10 **Abstract**

11 The results of a comprehensive study of submerged paleoenvironments developed along the
12 karstified eastern Adriatic coast during the Late Quaternary are presented in this study. The Lošinj
13 Channel is a drowned karst basin filled with sediments. A multi-proxy analysis of two sediment cores
14 (LK-12 and LK-15) recovered from water depths of 62 and 64 m was conducted. We used magnetic
15 susceptibility, grain size, mineralogy, XRF core scanning, organic and inorganic carbon, total nitrogen,
16 and paleontological data, supplemented with AMS ¹⁴C dating results and high-resolution seismic data,
17 to reconstruct the infill history of the Lošinj basin during the Late Pleistocene and Holocene. Our
18 findings include the first detailed description of the presumed Marine Isotope Stage (MIS) 5a marine
19 sediment succession along the eastern Adriatic coast. Deposition in the brackish-to-freshwater
20 lacustrine body (Lošinj paleolake) occurred during MIS 3. Sea level lowstand that followed caused the
21 formation of environmental conditions typical of a karst polje. The post-Last Glacial Maximum (LGM)
22 sea level rise led to the establishment of a brackish marine lake with seawater seepage through the
23 karstified sill at 13.7 cal kyr B.P. The transition to the present-day marine conditions commenced at
24 10.5 cal kyr B.P. Paleoenvironmental changes in the investigated area can be linked to the presence of

25 a sill at -50 m depth that separates the Lošinj basin from the Kvarnerić Bay. The sill depth determines
26 the isolation or inundation of the investigated basin in response to the changes in sea level.
27 Paleoenvironments reacted sensitively to these changes, and therefore, the study area represents an
28 ideal setting to track regional sea level and climate variability.

29 **1. Introduction**

30 Submerged paleoenvironments formed during the Late Quaternary have been the focus of
31 many recent geological and archaeological studies in the Mediterranean region (e.g., Micallef et al.,
32 2013; Foglini et al., 2015; Geraga et al., 2017; Flemming et al., 2017). This type of research is essential
33 in estimating the response of present-day coastal areas to future sea level and climate changes
34 (Lambeck et al., 2011; Wahl et al., 2017; Antonioli et al., 2017). The Quaternary period is characterized
35 by significant sea level fluctuations primarily resulting from the waxing and waning of large high-
36 latitude ice sheets (Shackleton, 1987; Lambeck and Chappell, 2001). At regional and local scales, the
37 impact of glacio-hydro-isostasy and vertical tectonic movements is also relevant when assessing sea
38 level changes (Lambeck et al., 2004; Antonioli et al., 2009; Rovere et al., 2016). An exhaustive studies
39 of relative sea level (RSL) changes in the Mediterranean Sea were published by Sivan et al. (2001),
40 Lambeck et al. (2011), Vacchi et al. (2014, 2016), Benjamin et al. (2017) and references therein. It is
41 considered that during MIS 5a RSL was approximately 1 m higher than at present (Dorale et al., 2010).
42 However, there is a lack of Mediterranean MIS 4 and MIS 3 RSL records (Caruso et al., 2011; Benjamin
43 et al., 2017). Global data suggests that during MIS 3 sea level was between -60 and -90 m (Siddall et
44 al., 2003; Rohling et al., 2008). During the LGM sea level fell rapidly to reach a lowstand of -120 to -134
45 m (Fairbanks, 1989; Lambeck and Purcell, 2005; Lambeck et al., 2014). The post-LGM melting of the
46 ice sheets caused inundation of the coastal areas in the Mediterranean region and led to the
47 development of numerous present-day embayments, channels and indentations (Flemming et al.,
48 2017; Benjamin et al., 2017).

49 Considering the fact that the vast areas of the Adriatic Sea are very shallow (<100 m depth),
50 paleoenvironmental evolution was substantially influenced by the Late Quaternary sea level changes
51 (Bailey and Flemming, 2008). Paleoenvironments developed along the western and northern coast of
52 the Adriatic Sea have been thoroughly investigated, but there is an obvious scarcity of data regarding
53 the eastern Adriatic coast (Alberico et al., 2017).

54 The development of a large alluvial plain cut only by the Po River and its tributaries during the
55 sea level lowstands is well-documented in sedimentary and seismic records in the western and
56 northern part of the Adriatic Sea (e.g., Correggiari et al., 1996; Galassi and Marocco, 1999; Correggiari
57 et al., 2001; Kent et al., 2002; Amorosi et al., 2003; Amorosi et al., 2004; Amorosi et al., 2008; Moscon
58 et al., 2015; Campo et al., 2017; Trobec et al., 2017; Pellegrini et al., 2018; Ronchi et al., 2018). At times
59 of sea level rise, the alluvial plain was inundated, with the development of barrier-lagoon systems,
60 which allow tracking of the sea level rise in the region (e.g., Correggiari et al., 1996; Amorosi et al.,
61 2003; Moscon et al., 2015).

62 The research conducted so far along the eastern coast of the Adriatic Sea has indicated
63 different paleoenvironmental evolution of this area. The existence of submerged lacustrine
64 environments (paleolakes) along the eastern coast of the Adriatic Sea was suggested by Juračić et al.
65 (1999), who proposed the development of brackish or freshwater lacustrine environments during the
66 glacial sea level lowstands. Schmidt et al. (2001) and Wunsam et al. (1999) described the Last Glacial
67 and Holocene lacustrine deposits that preceded the onset of the marine deposition in the Valun Bay
68 in the Kvarner region and Mljet Lakes in the southern Dalmatia. Recent studies based on marine
69 sediment cores are mostly limited to the Holocene (Faivre et al., 2011; Marriner et al., 2014; Felja et
70 al., 2015; Shaw et al., 2016; Brunović et al., 2019). Research that encompasses a long-term high-
71 resolution Pleistocene sedimentary record is still missing. Data regarding RSL and climate variations in
72 the eastern Adriatic during the Pleistocene have been mostly derived from analysis of submerged

73 speleothems. Evidence of these changes is presented in the research published by Surić et al. (2005,
74 2009) and Surić and Juračić (2010).

75 The main aim of this study is to investigate how depositional environments along the eastern
76 Adriatic coast responded to the Late Pleistocene and Holocene sea level and climate changes. We
77 provide a sedimentological record based on two piston cores (LK-12 and LK-15), combined with high
78 resolution seismic data, from the submerged silled karst basin in the Lošinj Channel. It is considered
79 that sediments deposited in silled and partly isolated basins are valuable records of past environmental
80 and sea level changes (Lambeck and Purcell, 2005; Long et al., 2011). Prolific paleoenvironmental
81 studies of silled basins have been conducted in Canada and Greenland (Long et al., 2011; Normandeau
82 et al., 2017; Fedje et al., 2018), Scotland (Lloyd, 2000; Lloyd & Evans, 2002), Scandinavia (Balascio et
83 al., 2011; Narančić et al., 2016), and Black and Marmara Sea (Çağatay et al., 2003; Bahr et al., 2005;
84 Taviani et al., 2014; Filikci et al., 2017). There is, however, a lack of such studies in the Adriatic Sea.
85 Here, we evaluate the suitability of the submerged silled karst basin in the Lošinj Channel to improve
86 and fill the gaps in the Late Quaternary paleoenvironmental reconstructions along the eastern Adriatic
87 coast.

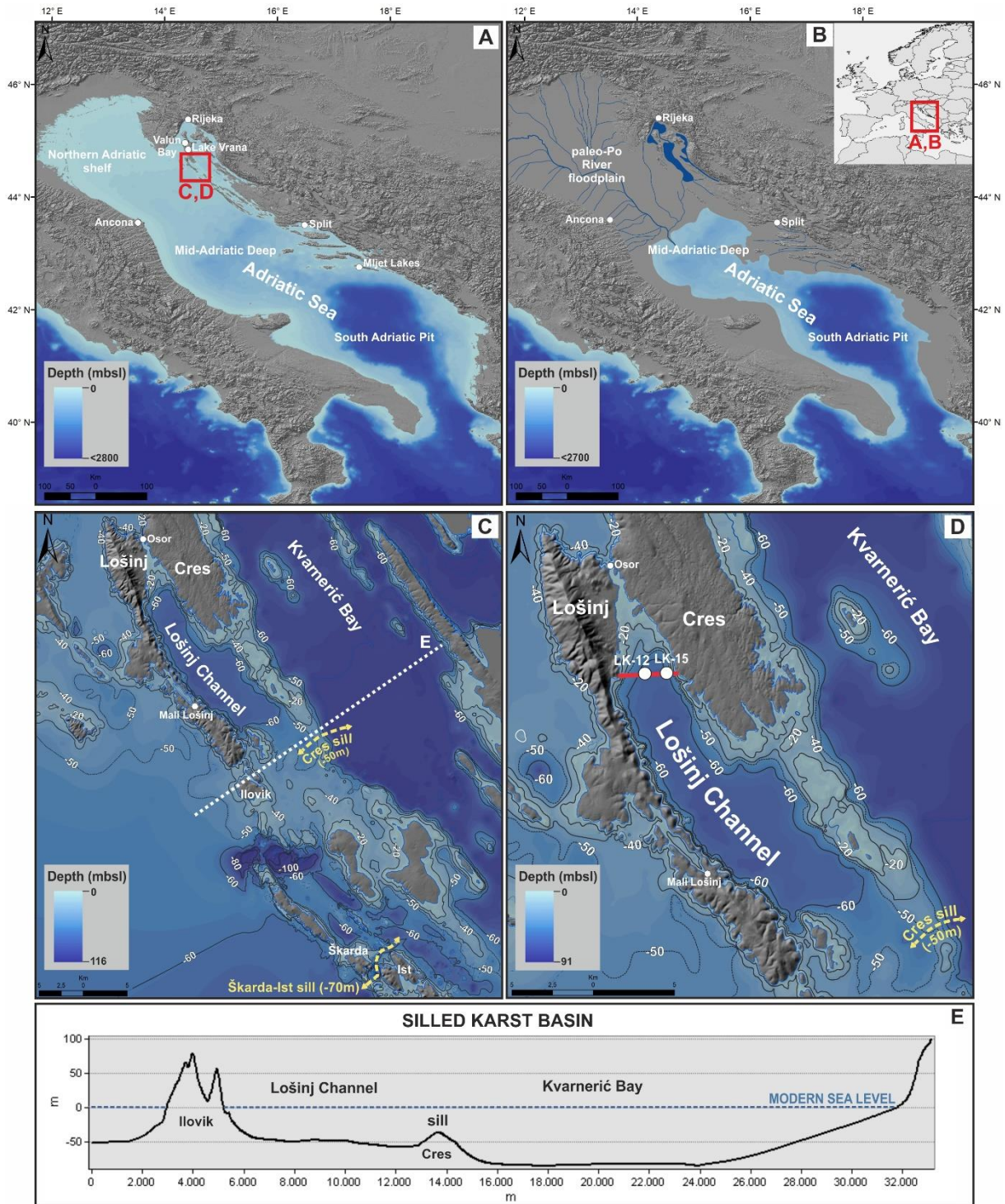
88 **2. Regional setting**

89 The Lošinj Channel encompasses a 35-km-long and 6-km-wide area between the shore-parallel
90 islands Lošinj and Cres on the eastern coast of the Adriatic Sea, in the Kvarner region (Fig. 1). The
91 Adriatic Sea is a part of the Mediterranean Sea and is characterized by its semi-enclosed nature. The
92 eastern and western coasts of the Adriatic Sea differ significantly (Pikelj and Juračić, 2013). Whereas
93 the eastern coast is described in the literature as a Dalmatian-type coast with chains of islands parallel
94 to the coastline and channels in between them (Kelletat, 2005), the western side is a typical low-lying
95 coast with dominant riverine sediment input (Frignani et al., 2005).

96 Carbonate deposits ranging in age from Carboniferous to Eocene predominantly build the
97 eastern Adriatic coast and islands (Vlahović et al., 2005). Prevalent strata on the islands Lošinj and Cres
98 are carbonate deposits of Cretaceous age (Korbar et al., 2001; Korbar and Husinec, 2003). Paleogene
99 carbonate deposits and Quaternary loess deposits are also present (Mamužić, 1968; Magaš, 1968;
100 Fuček et al., 2012; Fuček et al., 2014). Several reverse faults were recognized on geological maps of
101 islands Lošinj and Cres (Mamužić, 1968; Magaš, 1968). The reader is referred to Korbar (2009) and
102 references therein for a comprehensive overview of the eastern Adriatic tectonic setting. Neotectonic
103 history of the coast is complex and still a matter of debate, with different studies arguing subsidence
104 (Antonioli et al., 2009; Faivre et al., 2011; Marriner et al., 2014; Shaw et al., 2018; Faivre et al., 2019),
105 uplift (Surić et al., 2009, 2014) and tectonic stability (Faivre et al., 2013).

106 Because carbonate rocks are prone to karstification, different features typical for karst were
107 formed (dolines, poljes, caves, etc.). There were two major stages of karst development in the
108 Mediterranean, the Messinian Salinity Crisis and the Pliocene/Quaternary (Mocochain et al., 2006;
109 Roveri et al., 2014). Some of the karst features developed along the eastern Adriatic coast were
110 submerged due to the rising sea level during the Late Pleistocene-Holocene marine transgression that
111 shaped the present-day coast (Surić, 2002; Kelletat, 2005; Paskoff, 2005). The hydrogeology of the
112 karstified coastal environments is highly dependent on sea level oscillations considering that a rise in
113 sea level causes a rise in the groundwater level and seawater seepage through karstified and porous
114 rocks (Shinn et al., 1996; van Hengstum et al., 2011; van Hengstum and Scott, 2011).

115 The study area of the Lošinj Channel is a drowned silled karst basin (Fig. 1). Submerged
116 prolongation of the Island of Cres forms a sill (Cres sill), with the deepest point at -50 m, that separates
117 the Lošinj Channel from the Kvarnerić Bay (Fig. 1). The Cres sill depth determines the isolation or
118 flooding of the Lošinj Channel in relation to the Quaternary sea level changes. Seawater flooding of the
119 adjacent Kvarnerić Bay probably occurred through a narrow channel/sill at a depth of approximately
120 70 m located between the islands Škarda and Ist (Škarda-Ist sill) (Fig. 1C).



121

122 Fig. 1. Maps and cross-section of the investigated area. A) Map of the present-day Adriatic Sea. B)
 123 Schematic map of the Adriatic Sea during the LGM (western Adriatic coast is modified from Maselli et
 124 al., 2011 and Maselli and Trincardi, 2013; eastern Adriatic coast is reconstructed using bathymetry data
 125 (Becker et al., 2009) and data from Miko et al., 2016). C) Map of the Lošinj Channel and Kvarnerić Bay

126 with sill locations (yellow lines). D) Coring locations (white circles) and interpreted Seismic line 1 (red
127 line). E) Cross-section of the Lošinj Channel. The location of the cross-section is marked on map C.

128 **3. Materials and methods**

129 **3.1. High-resolution seismic survey**

130 High-resolution seismic data were obtained in April 2015 using a 3.5-kHz sub-bottom profiling
131 system with Geopulse transmitter and a 4 array transducer, mounted on the vessel *Zlatica dva*. A pulse
132 duration of 1 ms and a pulse rate of 10 s⁻¹ were used. The vertical resolution of the system was about
133 0.5 m which is the minimum distance between the distinguishable reflectors. The average survey speed
134 was 4 knots, and the positional data was provided by a Differential Global Positioning System (DGPS)
135 with an accuracy of ±1-2 m. Overall, almost 204 km of seismic lines were recorded during the seismic
136 survey in the Lošinj Channel. For this study, only the high-resolution seismic reflection profile (Seismic
137 line 1) along the coring sites was interpreted (Fig. 1).

138 **3.2. Sediment cores**

139 Two sediment cores (LK-12 and LK-15) were retrieved from the northern part of the Lošinj
140 Channel in September 2015 (Fig. 1). A coring platform equipped with a Niederreiter piston corer
141 (UWITEC®) was used for core extraction. Core LK-12 (422 cm) was extracted adjacent to the Island of
142 Lošinj (44°38'16" N, 14°25'10" E), whereas core LK-15 (480 cm) was retrieved in the vicinity of the
143 Island of Cres (44°38'16" N, 14°26'11" E). The cores were taken at water depths of 62 and 64 m,
144 respectively (Fig. 1).

145 **3.3. Sediment core analysis**

146 Sediment cores LK-12 and LK-15 were analyzed through a multi-proxy approach. In the
147 laboratory, cores were cut into approximately 1.5-m-long segments, split lengthwise, photographed
148 and stored at +4°C until further analysis.

149 **3.3.1. Magnetic susceptibility**

150 Manual measurements of magnetic susceptibility (MS) with a Bartington MS2E surface sensor
151 at 1-cm resolution were conducted on the working halves of the cores.

152 **3.3.2. Grain size**

153 The grain size analyses were carried out on 148 samples using a Shimadzu SALD-2300 laser
154 diffraction particle size analyzer. To analyze the grain size distribution of the siliciclastic component in
155 the carbonate-rich environment, it was necessary to remove both organic material with hydrogen
156 peroxide (H₂O₂) and carbonates with hydrochloric acid (HCl) (Murray, 2002). Furthermore, sodium
157 hexametaphosphate ((NaPO₃)₆) was added to the samples to prevent particle aggregation, whereas
158 larger mollusk shells were removed manually from the sediment prior to the pretreatment. Using the
159 GRADISTAT software package (Blott and Pye, 2001), main statistical parameters were determined
160 following the Folk and Ward (1957) method.

161 **3.3.3. Mineralogy**

162 Bulk mineralogical analyses were performed on selected powder samples taken throughout
163 the cores using an X'Pert Powder diffractometer (XRD) equipped with Ni-filter CuK α radiation, a vertical
164 goniometer with a θ/θ geometry, and a PIXcel detector. The scan conditions were set to 45 kV and 40
165 mA, alongside $\frac{1}{4}$ divergence and antiscatter slits, and with a step size of 0.02° 2 θ and a 4 s time per
166 step within a range between 4° 2 θ and 66° 2 θ .

167 **3.3.4. XRF core scanning**

168 The downcore relative elemental composition of sediment cores in 1 cm resolution was
169 analyzed at the Institute of Marine Science (CNR-ISMAR) in Bologna using an AVAATECH μ XRF core
170 scanner. Analysis of the elemental composition was performed using an X-ray source with the voltage

171 set to 10 and 30 kV, which enabled measurements of major and minor elements. The acquired XRF
172 scanning data are semi-quantitative and reported as elemental ratios (Croudace et al., 2006).

173 **3.3.5. Total organic and inorganic carbon and total nitrogen**

174 Total organic (TOC) and inorganic carbon (TIC) and nitrogen (TN) abundances in 157 samples
175 were determined using a Thermo Fisher Scientific Flash 2000 NC Analyzer. This method allows direct
176 measurements of the total carbon (TC) and TN. The addition of HCl removes the carbonate component
177 and allows the determination of TOC (Tung and Tanner, 2003). The difference between TC and TOC
178 was used for calculation of TIC, whereas the calcium carbonate (CaCO₃) content was calculated from
179 the obtained TIC values. The C/N ratio was calculated by dividing the TOC and TN.

180 **3.3.6. Paleontology**

181 To further strengthen the reconstruction of the past environments and to establish with
182 certainty the timing of marine intrusion into the Lošinj Channel, foraminiferal assemblages were
183 determined. Foraminifera are considered to be a useful tool for the reconstruction of
184 paleoenvironmental changes (e.g., Lloyd, 2000; Cosentino et al., 2017). In total, 32 samples in core LK-
185 12 were chosen for analysis. The benthic foraminifera specimens were observed under a binocular
186 microscope in the fraction >63 µm. Approximately 300 specimens were counted in each sample.
187 Samples with total number of foraminifera specimens <300 were also examined and specimens
188 counted. Identification of the genera and species is primarily based on the classifications given by
189 Cimerman and Langer (1991) and Loeblich and Tappan (1987). The purpose of this paper is not to
190 perform a detailed statistical analysis of foraminifera assemblages but rather to determine their
191 presence or absence. Determination of mollusk genera present in the sediment cores will further
192 improve the paleoenvironmental reconstruction.

193 **3.3.7. Core chronology**

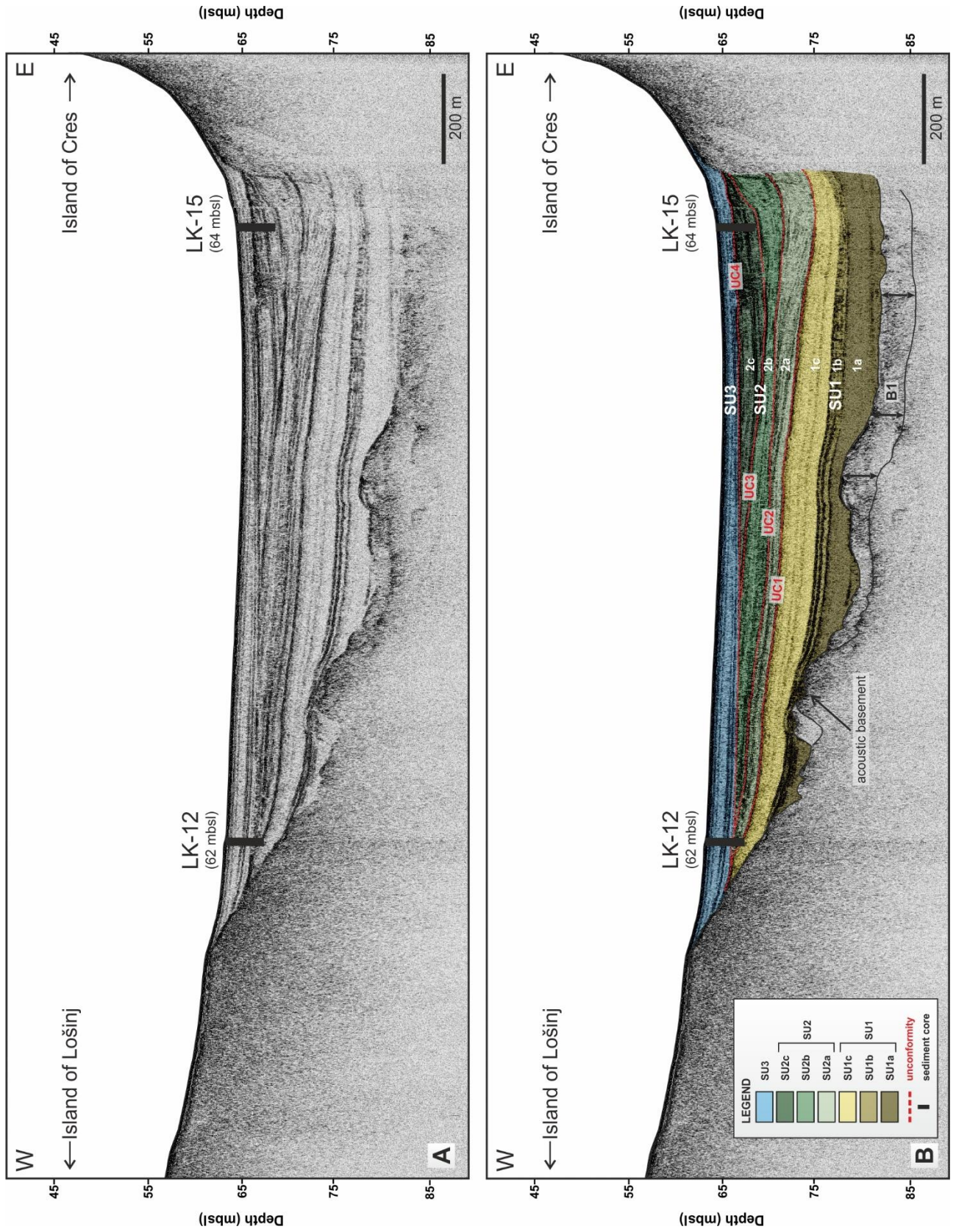
194 Core chronologies were established using the accelerator mass spectrometry (AMS)
195 radiocarbon dating method (^{14}C) at Beta Analytics Laboratory. For dating purposes, 10 mollusk shells
196 were selected from sediment cores LK-12 and LK-15. Terrestrial plant macrofossils and charcoal were
197 not present in the analyzed cores. The basal part of core LK-15 (from 135 cm downcore) was also
198 devoid of mollusk shells suitable for dating.

199 The radiocarbon data were further analyzed using Clam software package (Blaauw, 2010) to
200 obtain reliable age-depth models for each core. The marine reservoir age correction of 456 ± 46
201 ($\Delta R=100\pm 20$ ^{14}C yr) was adopted (Faivre et al., 2015). The ages obtained from the specimens of the
202 freshwater mollusk species *Bithynia tentaculata* were also corrected for marine reservoir effects due
203 to their stable isotopes shell values ($\delta^{13}\text{C}=-1.6\text{--}2.8$), which are typical for growth in the water with
204 marine influence (Stuiver and Polach, 1977). The Marine13 calibration curve was used for calibration
205 of the obtained data into calendar years (Reimer et al., 2013).

206 **4. Results**

207 **4.1. High-resolution seismic data**

208 The interpreted seismic profile (Seismic line 1) indicates the existence of a 22-m-thick
209 sedimentary succession at the coring sites (Fig. 2). Three main units (SU1-SU3) and six subunits (SU2a-
210 SU2c and SU3a-SU3c), bounded by unconformities (UC1-UC4), have been determined based on the
211 seismic unit definition proposed by Mitchum et al. (1977). The acoustic basement has a prolonged
212 acoustic character, whereas its upper part (B1) exhibits amorphous acoustic facies (Fig. 2). Directly
213 above the acoustic basement, unit SU1 has been recognized. Reflector characteristics within SU1 led
214 to the subdivision of seismic subunits SU1a to SU1c. Subunits SU1a and SU1c show a semi-transparent
215 acoustic character with a few parallel weak internal reflectors. SU1b consists of moderate-to-high
216 amplitude and laterally continuous reflectors (Fig.2). The lowermost unit SU1 is distinguished from unit
217 SU2 by a distinct unconformity (UC1). Unit SU2 consists of bands of sub-parallel inclined reflectors with
218 limited lateral continuity featuring high frequencies with moderate amplitudes. SU2 can be subdivided
219 into three subunits (SU2a, SU2b and SU2c) that are well defined by their internal seismic characteristics
220 and stratigraphic contacts. High amplitude stratigraphic unconformities (UC2, UC3 and UC4) mark the
221 boundary between these subunits and between the SU2 and the overlying unit. The uppermost unit
222 SU3 appears acoustically semi-transparent with weak parallel reflectors. Sub-bottom data revealed
223 variable thickness of seismic units in the western and eastern side of the Lošinj Channel, where the
224 sediment cores were extracted. Cores LK-12 and LK-15 penetrated through 3 previously described units
225 (SU3 and subunits SU2c and SU1c) (Fig. 2).



226

227 Fig. 2. (A) Seismic profile of Seismic line 1 and (B) its stratigraphic interpretation.

228 4.2. Sediment core data

229 4.2.1. Core chronology

230 Radiocarbon measurements on 8 mollusk shells revealed that sediment core LK-12 spans the
231 Late Pleistocene to Holocene time interval (Table 1). ^{14}C analysis of the mollusk shells from the lower
232 part of the core (329 and 259 cm) yielded ages of approximately 46.5 and 45 cal kyr B.P. The LK-15
233 sediment core chronology is less constrained with 2 dates that indicate Holocene age of the upper core
234 section (10.3 cal kyr B.P. and 9.6 cal kyr B.P.) (Table 1).

235 Table 1. AMS ^{14}C dating results of samples from sediment cores LK-12 and LK-15.

Sediment core	Depth (cm)	Sample ID	Material	$\delta^{13}\text{C}$ (‰)	Conventional radiocarbon age (^{14}C B.P.)	Probability (%)	Calibrated age (cal B.P.)
LK-12	37	Beta - 475881	gastropod shell	+3.0	5550 ± 30	94.2	5725-5909
LK-12	201	Beta - 475882	bivalve shell	+0.8	9680 ± 30	95	10272-10486
LK-12	204	Beta - 459905	gastropod shell	+2.0	9750±30	95	10411-10572
LK-12	211	Beta - 459907	gastropod shell	+0.1	11750± 30	95	13079-13225
LK-12	223	Beta - 468184	gastropod shell	-0.6	12210±40	95	13469-13689
LK-12	233	Beta - 475880	gastropod shell	-1.6	12310±40	95	13577-13758
LK-12	259	Beta - 468185	gastropod shell	+2.8	42110±630	95	44040-45980
LK-12	329	Beta - 459906	gastropod shell	0.0	43050±830	95	45032-47982
LK-15	83	Beta - 468186	bivalve shell	+1.8	9040 ± 30	95	9484-9672
LK-15	134	Beta - 468187	gastropod shell	+3.0	9590 ± 30	92.7	10205-10429

236

237 4.2.2. Core lithology and multi-proxy analysis

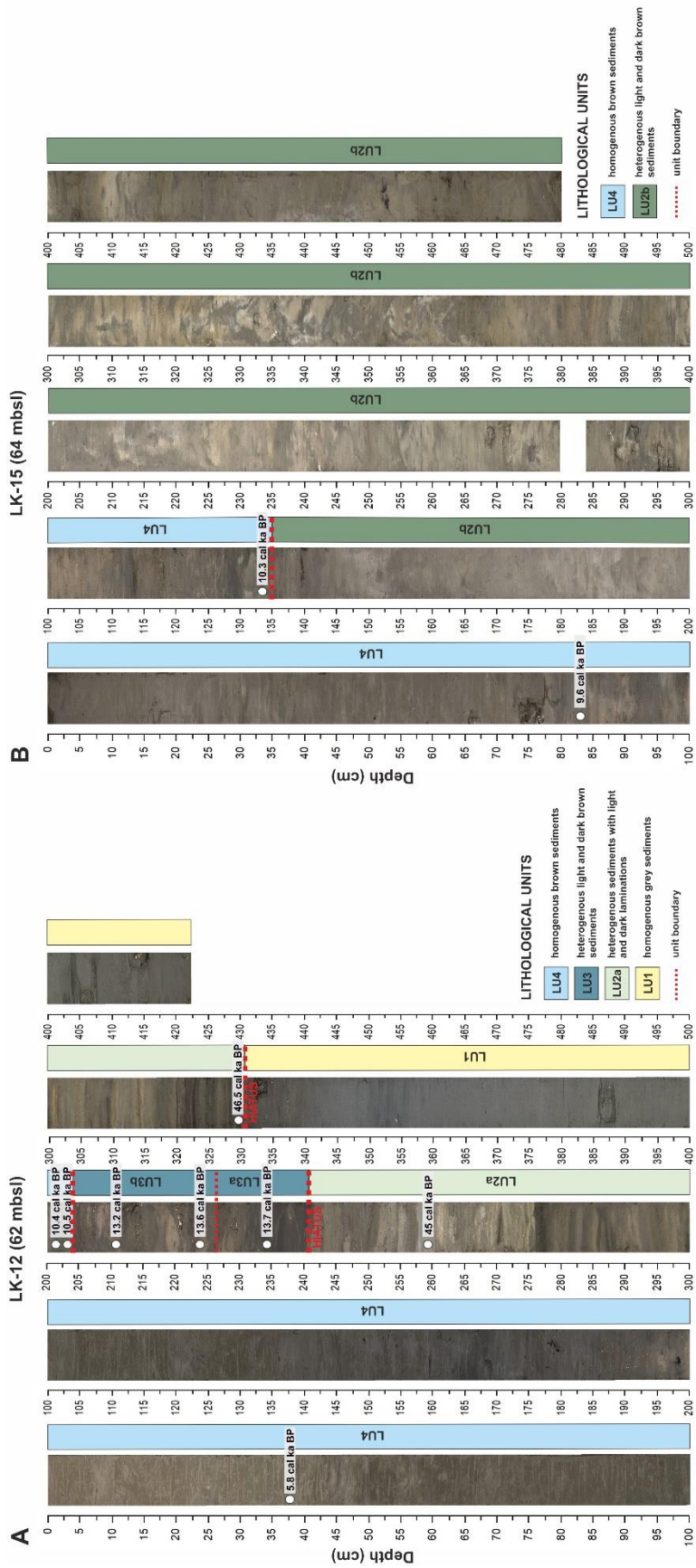
238 Sedimentological, geochemical, mineralogical, and paleontological data used in this study
239 enabled the division of cores LK-12 and LK-15 into distinct lithological units (Fig. 3).

240 Sediment core LK-12 was subdivided into four lithological units (Fig. 3). Homogenous grey
241 sediments of the lowermost lithological unit LU1 (>46.5 cal kyr B.P.), recognized in the interval from
242 422 to 329 cm, are predominantly constituted of high percentages of silt-sized particles (77-84%) (Fig.
243 4; Supplement 1). Magnetic susceptibility is low in this unit ($2.9\text{-}13.7 \times 10^{-5}$ SI), whereas the main
244 mineralogical constituents of the bulk samples are quartz, dolomite, calcite and aragonite. The
245 lowermost part of core LK-12 is characterized by high Sr/Ca and Ti/Ca ratios (Fig. 4). The TOC content
246 (0.42-0.97%) and C/N ratios (7.95-13.57) are low. The CaCO₃ content vary between 41.61-56.43% (Fig.
247 4; Supplement 2). Benthic foraminiferal assemblages are dominated by species *Aubignyna planidorso*,
248 *Elphidium translucens* and *Ammonia tepida*. The relative abundances of foraminifera specimens are
249 provided in Supplement 3. Recognized mollusks include *Cerastoderma* sp., *Turritella* sp. and *Cerithium*
250 sp. Significant number of fragmented shells was observed.

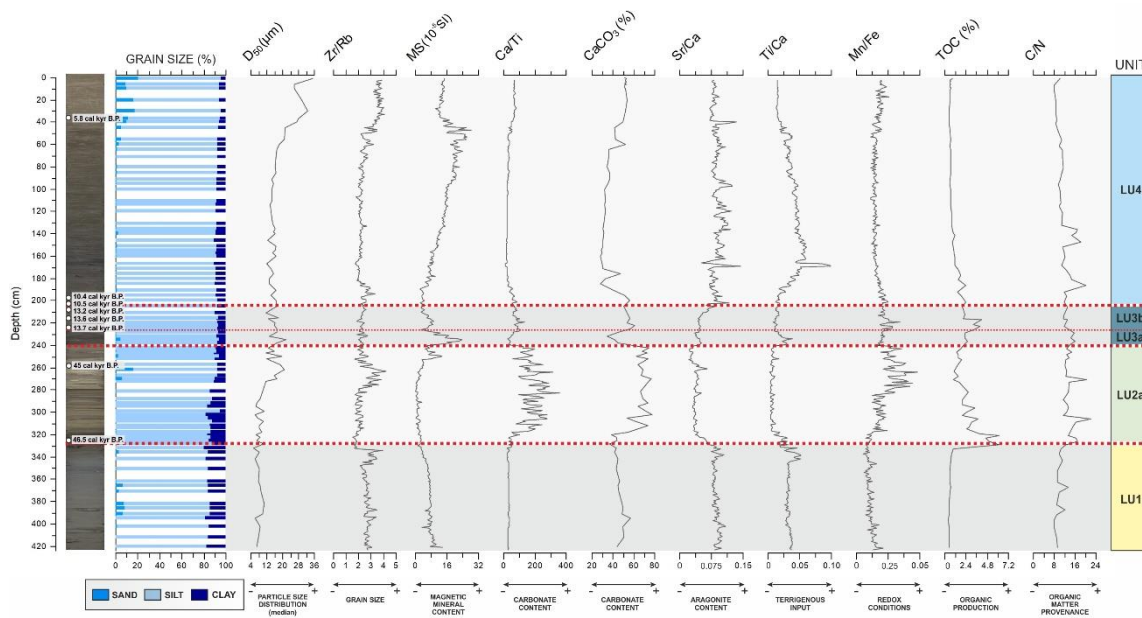
251 Sediments of the overlying unit LU2a in core LK-12 (329-240 cm; 46.5-44.7 cal kyr B.P) are
252 distinguished by light and dark brown laminations (Fig. 3). This unit is characterized by a slightly coarser
253 grain size and low MS ($0.2\text{-}13.6 \times 10^{-5}$ SI) (Fig. 4). Calcite predominantly builds sediments from LU2a,
254 whereas quartz and dolomite are less abundant. The acquired XRF data exhibit an increase in Ca/Ti
255 and a decrease in Sr/Ca ratios in LU2a. The Mn/Fe ratios abruptly increase in the interval from 277 to
256 240 cm. The Zr/Rb ratios reached maximum in the core interval from 286 to 254 cm (Fig. 4). The lower
257 part of unit LU2a (329-281 cm) is composed of organic-rich sediments, with TOC content of up to 6.18%
258 (Fig. 4). The upper part of this unit (281-240 cm) has a lighter color and is dominated by high CaCO₃
259 content (up to 77.7%). The C/N ratios vary between 11.36-22.19 (Fig. 4; Supplement 2). Foraminiferal
260 analysis of 9 samples revealed poor preservation of foraminifera specimens and their low abundances.
261 The exception is the sample from the core depth of 260-261 cm, in which a low number of well-
262 preserved foraminifera specimens was observed. The mollusk fauna are dominated by *Bithynia*
263 *tentaculata*. In the basal part of this unit, *Chara oogonia* are especially abundant.

264

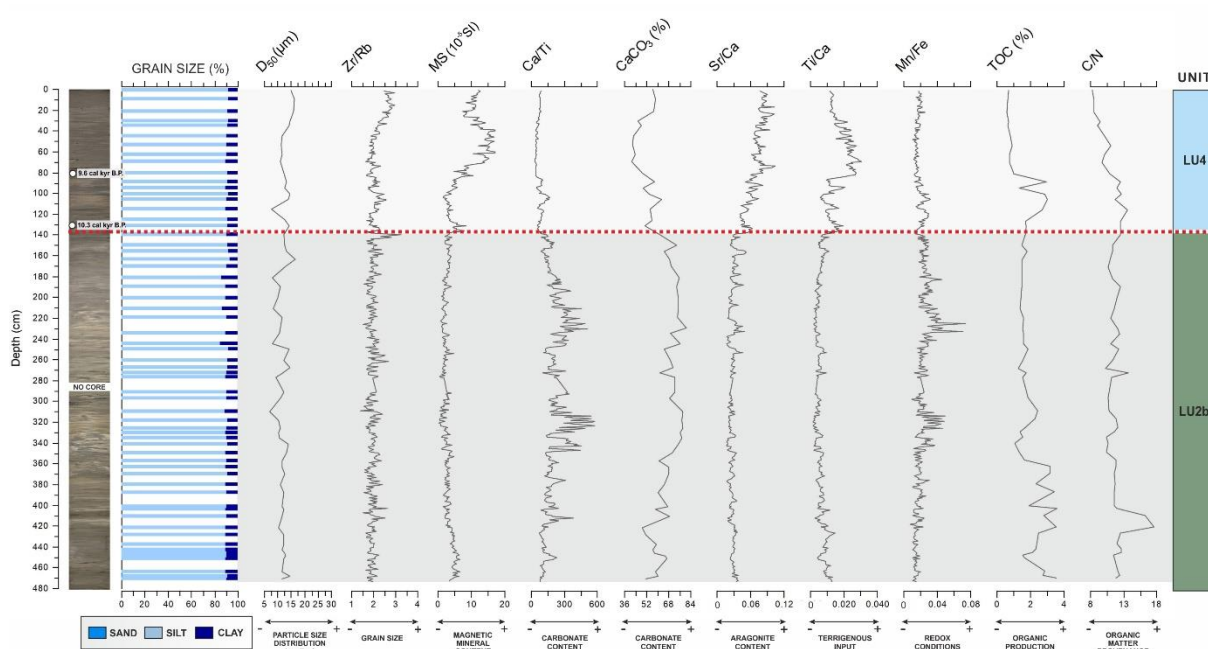
265 Fig. 3. Recognized lithological units in: A) sediment core LK-12, B) sediment core LK-15.



266 The third lithological unit LU3 is recognized in the core interval from 240-204 cm. Sediments
 267 from LU3 were deposited from 13.7 cal kyr B.P. to 10.5 cal kyr B.P. In the dark brown faintly-laminated
 268 sediments, silt-sized particles predominate (89-93%) (Fig. 4; Supplement 1). Quartz is the dominant
 269 mineral phase in all analyzed samples. Aragonite, calcite and dolomite were also determined.
 270 Significant variations in the obtained data enabled the differentiation of subunits LU3a and LU3b. High
 271 MS (up to 23.6×10^{-5} SI) was measured in the basal part of the unit (LU3a), whereas Ti/Ca ratios were
 272 also high. Fig. 4 demonstrates that after peaking in LU3a, C/N ratios decreased in LU3b (11.49-16.08).
 273 Towards the upper subunit, Ca/Ti, Sr/Ca and Mn/Fe ratios increased (Fig. 4). Subunit LU3b is
 274 characterized by CaCO₃ content of up to 60.9%, and higher TOC (2-4.2%) (Fig. 4; Supplement 2). A low
 275 number of foraminifera specimens -but in a good preservational state- were observed throughout unit
 276 LU3. Subunit LU3b is dominated by almost-monospecific foraminifera assemblages, composed of
 277 *Ammonia tepida* and *Criboelphidium gunteri* (Supplement 3). Mollusks *Theodoxus* sp., *Bithynia*
 278 *tentaculata*, *Turritella* sp. were recognized.



279
 280 Fig. 4. Downcore variability of grain size, MS, elemental ratios obtained using XRF core scanner, TOC
 281 and CaCO₃ content, and C/N ratios in sediment core LK-12.



282
 283 Fig. 5. Downcore variability of grain size, MS, elemental ratios obtained using XRF core scanner, TOC
 284 and CaCO₃ content, and C/N ratios in sediment core LK-15.

285 Sediments of the topmost unit LU4 in core LK-12 (204-0 cm), deposited from 10.5 cal kyr B.P.
 286 to the present, were distinguished by its brown color and coarsening-upwards succession (Fig. 4).
 287 Significant percentages of sand fraction were measured (up to 20%), in comparison with the previously
 288 described units. Lithological unit LU4 is characterized by an evident increase in MS ($2.5\text{-}28.3 \times 10^{-5}$ SI),
 289 as shown in Fig. 4. The dominant mineral phase is quartz, whereas calcite, aragonite and dolomite are
 290 also abundant. The Sr/Ca ratios exhibit an abrupt transition from unit LU3 into LU4 (Fig. 4). A peak in
 291 Ti/Ca ratio was observed at 168 cm, followed by a decrease towards the top of the core. A significant
 292 variations of C/N ratios were detected (7.95-23.57), whereas TOC content was generally low
 293 throughout the unit (0.49-2.4%). From 206 cm (transition LU3/LU4) foraminifera abundances increase.
 294 The assemblages are composed of *Elphidium translucens*, *Epistominella exuiga*, *Asterigerinata*
 295 *adriatica* and *Textularia conica* specimens (Supplement 3). Mollusks *Mytilus* sp. and *Cerastoderma* sp.
 296 were recognized.

297 Sediment core LK-15 was subdivided into two lithological units (Figs. 3 and 4). Differentiated
 298 units in sediment cores LK-12 and LK-15 are challenging to correlate, with the exception of the topmost

299 unit, because they have been deposited in different settings as evidenced by seismic data (Fig. 2). The
300 similarities in the sediment composition of the topmost unit LU4, in cores LK-12 and LK-15, can be
301 observed in Figs. 4 and 5. However, LU4 is less thick in core LK-15 (135-0 cm), and encompasses a
302 shorter time interval (10.3 cal kyr B.P.-present). Sediments of units LU1 and LU3, recognized in core
303 LK-12, are missing in core LK-15. However, additional lithological unit (LU2b) was distinguished in core
304 LK-15. There are certain similarities in the geochemical composition of this unit and lithological unit
305 LU2a from sediment core LK-12.

306 Faint laminations and possible dewatering structures were recognized in sediments from the
307 lowermost unit LU2b in core LK-15 (480-135 cm). Generally, silty sediments are characterized by high
308 Ca/Ti ratios and CaCO₃ content (up to 80.52%). Occasionally, pebble-sized carbonate clasts were
309 embedded in a matrix. The main mineralogical constituent of LU2b sediments is calcite. Both TOC
310 content (1.06-3.6%) and C/N ratios (10.32-17.55) are relatively high (Fig. 5). This unit is devoid of
311 macrofossils, apart from the poorly preserved gastropod shell at a core depth of 392 cm.

312 **5. Discussion**

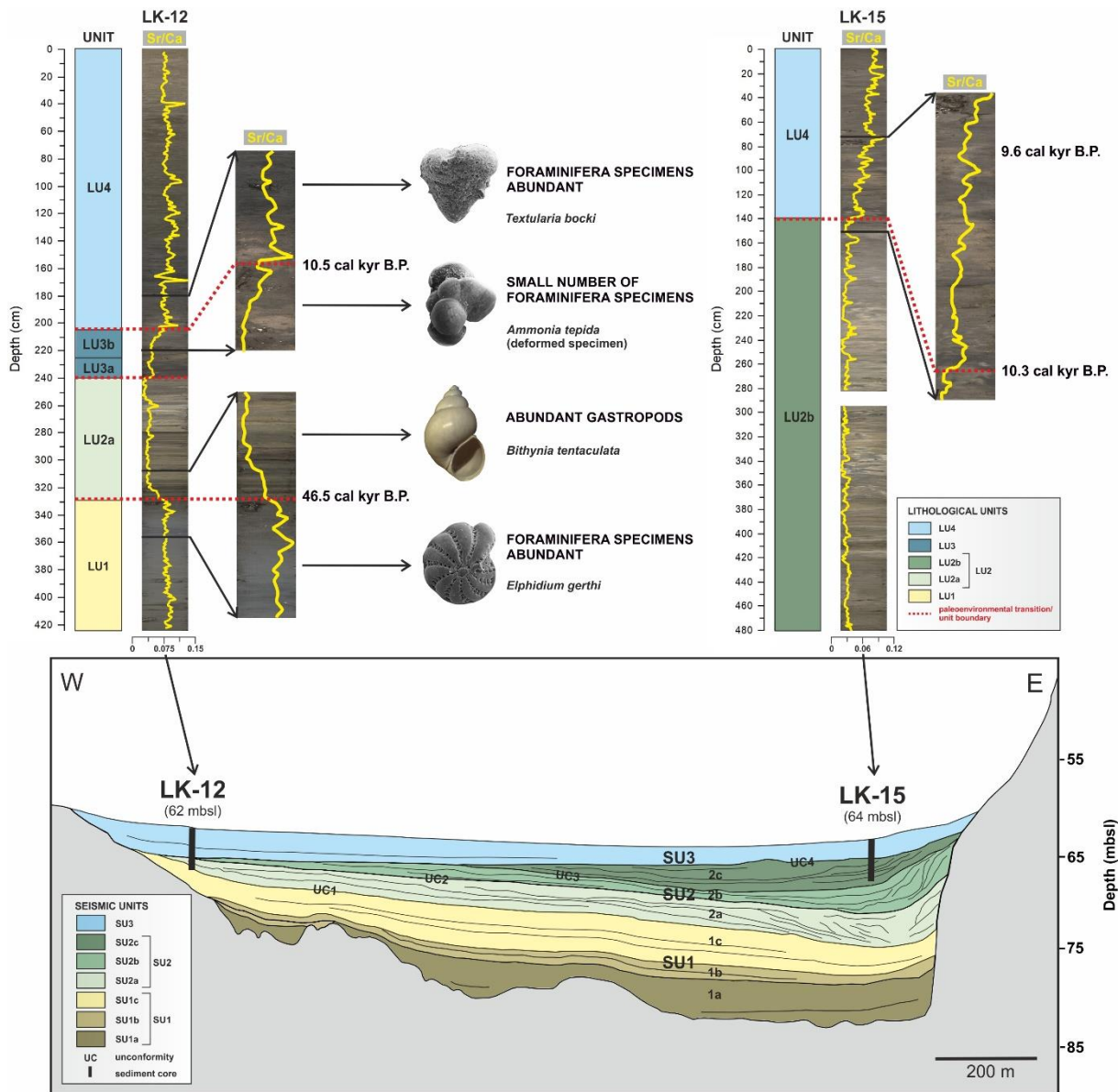
313 The sediment infill preserved in the Lošinj Channel karst basin reveals a dynamic depositional
314 history of the study area during the Late Pleistocene and Holocene. The comparison of all results
315 obtained via multi-proxy analysis of sediment cores LK-12 and LK-15 and correlation with seismic data
316 enabled the unravelling of this history. The dated sediment succession can be divided into several
317 paleoenvironmental phases primarily governed by climate changes, sea level oscillations, and basin
318 geomorphology of the study area. Each paleoenvironmental phase will be discussed below considering
319 (i) conditions in the depositional environment inferred from seismic and sediment core data (ii) global
320 and RSL changes in relation to the depth of the Cres sill.

321 **5.1. Marine phase (>46.5 cal kyr B.P.)**

322 **5.1.1. Paleoenvironmental reconstruction based on seismic and core data**

323 Sediments that were deposited at the bottom of the silled basin were not penetrated by
324 sediment cores (Fig. 2). Therefore, in this paper, we will not discuss the paleoenvironmental history of
325 the Lošinj Channel during the deposition of sediments from seismic subunits SU1a and SU1b. The
326 overlying acoustically semi-transparent seismic subunit SU1c onlaps (marine onlap) onto the acoustic
327 basement in the western part of the basin. Carbonate rocks that occur on the surrounding islands
328 constitute the acoustic basement, whereas the upper part of the acoustic basement (B1) exhibits
329 amorphous acoustic facies representing karstified carbonates (Fig. 2). As evidenced by the core-to-
330 seismic correlation, subunit SU1c corresponds to the basal part of the sediment core LK-12 (LU1) (Fig.
331 6 and Table 2). Several analyzed parameters in lithological unit LU1 show distinctive patterns, based
332 on which we were able to interpret the paleoenvironmental conditions in the Lošinj karst basin during
333 the deposition of sediments from this unit. The carbonate content is moderate to high throughout the
334 succession, emphasizing both marine and karst influence. However, the most important geochemical
335 feature of LU1 is the high Sr/Ca ratio, which can be used as a proxy of shallow marine environmental

336 conditions in the study area (Figs. 6 and 7A). The Sr-enriched seawater enables the precipitation of
337 aragonite in marine environment, contributing to the high Sr/Ca ratios (Croudace et al., 2006; Goudeau
338 et al., 2014; Filikci et al., 2017; Çağatay et al., 2019). The presence of aragonite in this interval is also
339 supported by XRD. Indicators for terrestrially sourced lithogenic material (e.g., Ti/Ca) (Bahr et al., 2005;
340 Blanchet et al., 2013; Croudace and Rothwell, 2015) show significant input of siliciclastics from soil
341 erosion from the catchment into the Lošinj basin (Figs. 4 and 7B). This is also evidenced by relatively
342 high MS (Fig. 4). The obtained data suggest that despite the prevalence of marine conditions, input of
343 terrestrially sourced material, possibly as a result of humid climate conditions and/or proximity of the
344 coring location to the coast, was important. The Mn/Fe ratio is frequently used as a proxy of redox
345 conditions (Haenssler et al., 2014; Croudace and Rothwell, 2015). The low values of Mn/Fe in LU1 likely
346 indicate that the Lošinj basin was not a fully oxygenated environment. We believe that in this unit,
347 Mn/Fe could be used as a proxy of redox conditions due to the poor correlation of Mn and terrestrial
348 elements (e.g., Ti) and Mn and trace metals (e.g., Zn) (Fig. 7C,D). Therefore, the existence of an
349 enclosed marine environment with limited water circulation due to the presence of the submerged sill
350 is postulated (Figs. 8A and 9A). Density stratification, and resulting anoxic conditions, in silled marine
351 basins has been reported and described in environmental studies of the enclosed Black Sea (Major et
352 al., 2002; Aksu et al., 2002). In the established marine environment in the Lošinj basin productivity was
353 low (<TOC), whereas preserved organic matter was aquatically sourced (<C/N; Meyers, 1994; Meyers,
354 2003; Lamb et al., 2006). Diverse foraminiferal assemblages and rich marine molluscan fauna support
355 the existence of marine environmental conditions (Fig. 6). The dominant foraminifera species
356 *Aubignyna planidorso*, *Elphidium translucens* and *Ammonia tepida* usually inhabit shallow marine-to-
357 brackish water environments (Murray et al., 2000; Debenay and Guillou, 2002; Murray, 2006).



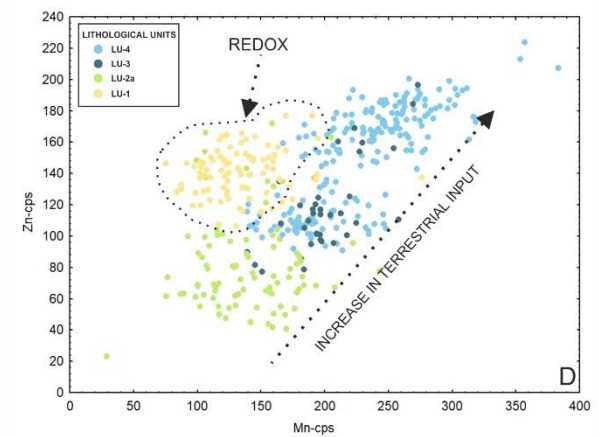
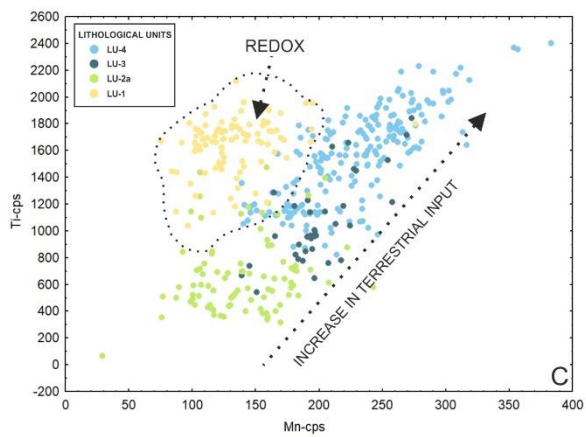
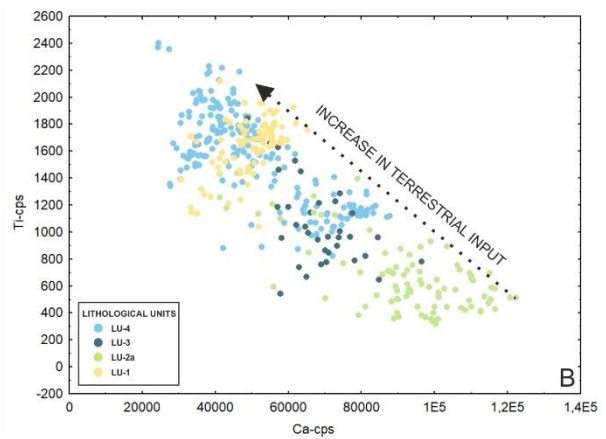
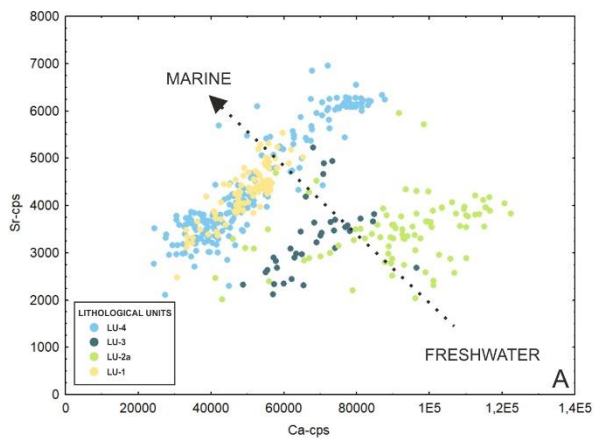
358

359 Fig. 6. Illustration of seismic and lithological units. Variations in Sr/Ca ratios in sediment cores LK-12
 360 and LK-15 are plotted and main paleontological components of differentiated units are shown.

361 Table 2. Correlation of recognized seismic and lithological units.

Seismic unit and unconformity	Seismic subunit	Lithological unit	Lithological subunit	Core depth	Stage/Epoch	Depositional environment	Figs. 8,9
SU1	a				Pleistocene		
	b				Pleistocene		
	c	LU1		LK-12 (422-329 cm)	MIS 5a	MARINE ENVIRONMENT	A
UC1		HIATUS			MIS 4	KARST POLJE	B
SU2	a	LU2	a	LK-12 (329-240 cm)	MIS 3	LACUSTRINE ENVIRONMENT	C
UC2		HIATUS					
SU2	b						
UC3		HIATUS			MIS 3/MIS 2	KARST POLJE	D
SU2	c	LU2	b	LK-15 (480-135 cm)			
UC4		HIATUS					
SU3		LU3	a	LK-12 (240-226 cm)	MIS 2	MARSH OR SHALLOW LAKE	E
			b	LK-12 (226-204 cm)		MARINE LAKE	E
		LU4		LK-12 (204-0 cm)	MIS 1	MARINE ENVIRONMENT	F, G
				LK-15 (135-0 cm)			

362



363

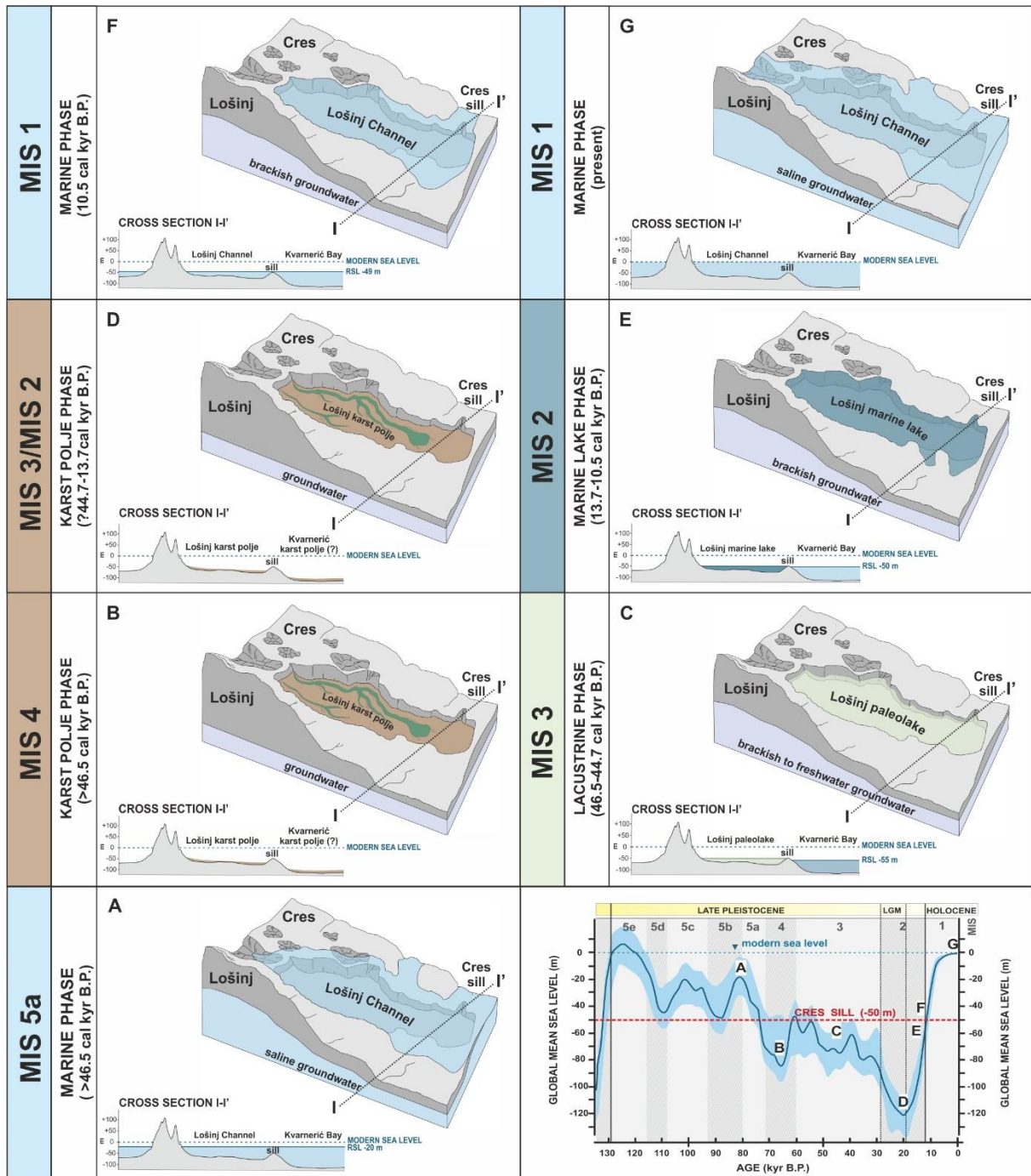
364 Fig. 7. Scatterplots of A) Ca (cps) against Sr (cps), B) Ca (cps) against Ti (cps), C) Mn (cps) against Ti (cps),
365 D) Mn (cps) against Zn (cps). Sediment core LK-12 was subdivided into units representing different
366 depositional environments: LU1- marine; LU2a- lacustrine; LU3- marine lake; LU4-marine.

367 **5.1.2 Paleoenvironmental reconstruction considering sea level fluctuations and sill depth**

368 The age of the described marine succession can only be hypothesized. The base of the
369 overlying unit LU2a in sediment core LK-12 has been dated at 46.5 cal kyr B.P. (MIS 3). Therefore, the
370 deposition of marine sediments corresponding to seismic subunit SU1c and lithological unit LU1
371 occurred before that time. It is possible that sediments were deposited during the older MIS 3, MIS 4
372 or MIS 5. However, for marine environmental conditions to develop in the Lošinj Channel, RSL needs
373 to be > -50 m, which corresponds to the deepest point of the present-day Cres sill that separates the
374 Lošinj Channel from the Kvarnerić Bay. It is considered that sea level was > -50 m only during MIS 5,
375 based on global and regional sea level data for this period (Waelbroeck et al., 2002; Dorale et al., 2010).
376 Previously conducted research in the Kvarner region by Surić et al. (2009) reported 2 sea level
377 highstands during MIS 5a. The sea level was higher than -14.5 m from 87-82 kyr, whereas from 90-82
378 kyr and from 77-64 kyr RSL was higher than -18.8 m. Therefore, we propose the deposition of the
379 described marine succession during the youngest part of MIS 5 (MIS 5a) (Figs. 8A and 9A). Surić et al.
380 (2009, 2014) also stressed possible tectonic activity in the region. In the case in which the Kvarner area
381 was indeed affected by tectonic uplift since MIS 5a, the Cres sill was possibly also uplifted. However,
382 the study area where uplift rates were estimated (Island of Krk) has a different tectonic setting
383 compared to the area investigated in the present study (Korbar, 2009). Therefore, uplift rates have not
384 been applied and further research regarding the tectonic setting of the Kvarner region must be
385 conducted to fully comprehend possible tectonically triggered variations in the Cres sill depth that had
386 a fundamental impact on the flooding or isolation of the Lošinj basin during the Quaternary. We
387 emphasize our uncertainty in the estimation of the age of the marine succession due to the inability

388 to date material, and the proposed MIS 5a age should be interpreted cautiously until substantiated
389 with additional evidence.

390 Whereas MIS 5a deposits have been investigated in the western and central Adriatic (Amorosi
391 et al., 2004; Ridente et al., 2008; Piva et al., 2008), marine deposits attributed to the MIS 5a have not
392 been found along the eastern coast of the Adriatic Sea so far. It appears that the possible deposition
393 of MIS 5a sediments deep in the subsurface of the Lošinj Channel is not necessarily a consequence of
394 subsidence but rather a peculiar geomorphological setting, with a generally steep coast and deep karst
395 depressions that accumulate sediments. The same can be hypothesized for MIS 5e marine deposits,
396 which have not yet been recorded with certainty along the eastern Adriatic coast (Babić et al., 2012).
397 If during this time period sea level was above the present level in the study area, MIS 5e deposits were
398 accumulated at the bottom of the deep karst depressions and potentially in the coastal area. However,
399 subsequent erosion events could have eroded coastal MIS 5e deposits during the latter lowstand
400 periods.



401

402

403

404

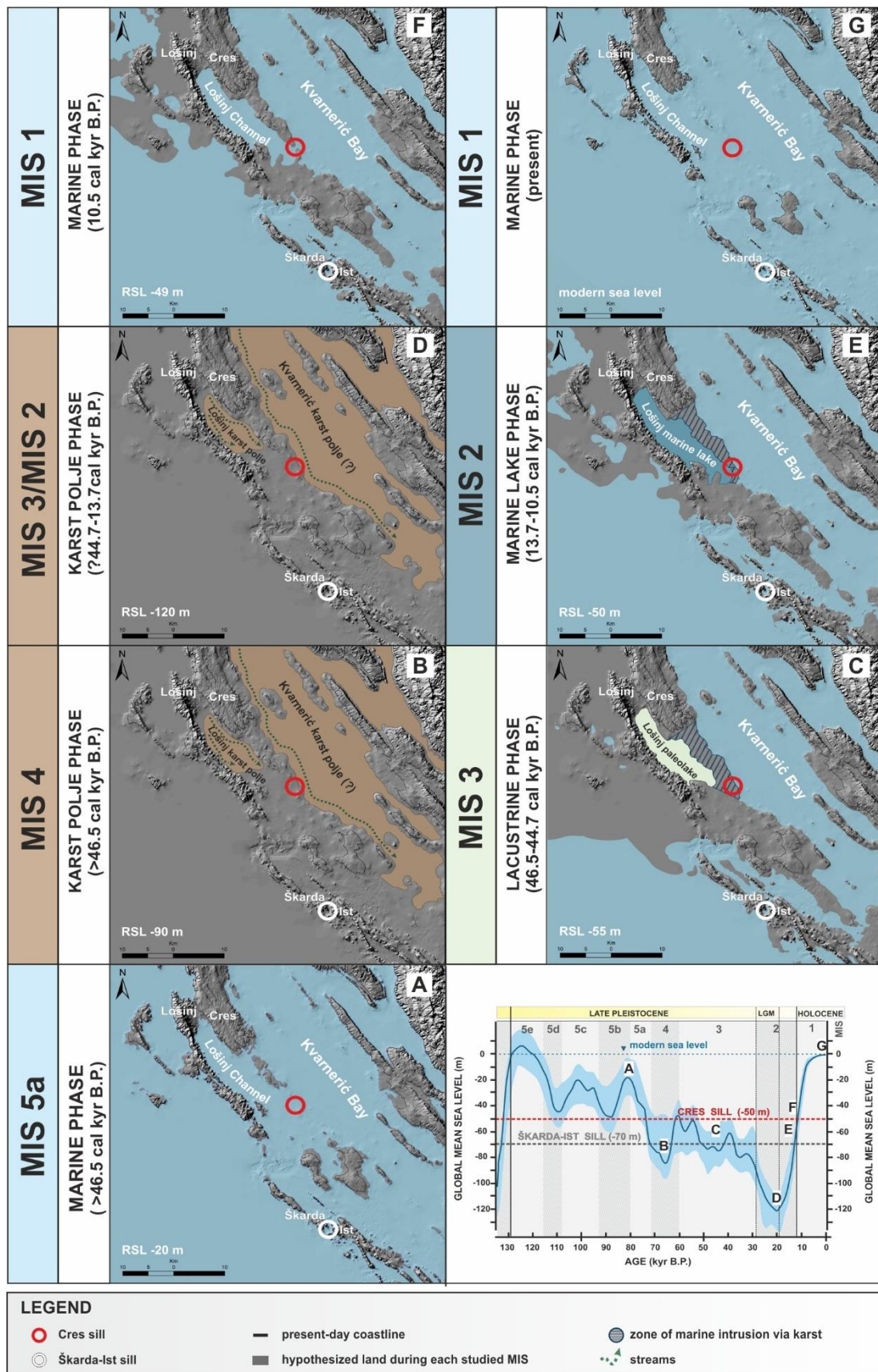
405

406

407

Fig. 8. Schematic paleoenvironmental reconstructions of the Lošinj Channel karst basin during the Late Pleistocene and Holocene and schematic cross-sections of the Lošinj basin with a marked connection to the Kvarnerić Bay RSL. A) MIS 5a marine environment. B) MIS 4 karst polje. C) MIS 3 Lošinj paleolake. D) MIS 3/MIS 2 karst polje phase with periodical streams. E) Lošinj marine lake during MIS 2 (Allerød interstadial). F) Seawater flooding of the Lošinj marine lake at 10.5 cal kyr B.P. G) Holocene marine environment. Each environmental phase is marked with corresponding letter on the Middle

408 Pleistocene-Holocene eustatic sea level curve (Waelbroeck et al., 2002; modified from Benjamin et al.,
409 2017).



410

411 Fig 9. Schematic Late Pleistocene and Holocene palaeogeographic maps of the Lošinj Channel karst

412 basin, based on bathymetric data (Tk25 topographic map to the scale 1:25 000, State Geodetic

413 Administration-Croatia), global sea level curve (Waelbroeck et al., 2002) and data from this study. A)
414 MIS 5a marine environment (with hypothesized RSL at -20 m). B) MIS 4 karst polje (with hypothesized
415 RSL at -90 m). C) MIS 3 Lošinj palaeolake (with hypothesized RSL at -55 m). D) MIS 3/MIS 2 karst polje
416 with periodical streams (with hypothesized RSL at -120 m). E) Lošinj marine lake during MIS 2 (Allerød
417 interstadial) (with hypothesized RSL at -50 m). F) Seawater flooding of the Lošinj marine lake at 10.5
418 cal kyr B.P (with hypothesized RSL at -49 m). G) Holocene marine environment (modern sea level). The
419 red circle marks the location of the Cres sill (-50 m). The white circle marks the location of Škarda-Ist
420 sill (-70 m). Each environmental phase is marked with corresponding letter on the Middle Pleistocene-
421 Holocene eustatic sea level curve (Waelbroeck et al., 2002; modified from Benjamin et al., 2017).

422 **5.2. Karst polje phase (>46.5 cal kyr B.P.)**

423 **5.2.1. Paleoenvironmental reconstruction based on seismic and core data**

424 An erosion event has been observed in the seismic data in the form of the strong reflector
425 (UC1) between seismic units SU1 and SU2 (Fig. 2). In sediment core LK-12, this event could be detected
426 as a very sharp contact between 2 different lithologies (units LU1 and LU2a) (Fig. 6).

427 **5.2.2. Paleoenvironmental reconstruction considering sea level fluctuations and sill depth**

428 Without a precise core chronology, it is difficult to estimate the existence and nature of this
429 hiatus. It is possible that the UC1 is related to the MIS 4 lowstand. During this stage, the sea level was
430 approximately 80-90 m lower than at present (Rohling et al., 2014), which could have caused the drop
431 in the groundwater level and the development of a terrestrial environment in the investigated area
432 (Lošinj karst polje) (Figs. 8B and 9B). Similar karst forms are present today along the eastern Adriatic
433 coast (Ford and Williams, 2007; Bonacci, 2013; Kranjc, 2013).

434 **5.3. Lacustrine phase (46.5-44.7 cal kyr B.P.)**

435 **5.3.1. Paleoenvironmental reconstruction based on seismic and core data**

436 Both seismic (subunit SU2a) and LK-12 core data (unit LU2a) provided clear evidence of a
437 distinctly different depositional environment at 46.5 cal kyr B.P., compared to the previously described
438 marine succession (Fig. 6). Geometry of the bands of the reflectors of SU2a implies the deposition of
439 layered sediments with different lithologic properties. The general increases in CaCO_3 and Ca/Ti, with
440 the dominant presence of calcite as the primary carbonate phase in lithological unit LU2a, is indicative
441 of the development of the lacustrine environment (Lošinj paleolake). High carbonate content is
442 common for deposition in karst lakes (Valero-Garcés et al., 2014; Hajek-Tadesse et al., 2018; Ilijanić et
443 al., 2018). The cessation of marine conditions is also supported by a strong decrease in the Sr/Ca ratios
444 (Fig. 6).

445 Smaller variations in certain geochemical proxies reveal the existence of somewhat different
446 environmental conditions at the onset and end of the recorded lacustrine phase (Fig. 4). First, dark and
447 laminated sediments were dominated by terrestrial organic matter. The significant increase in TOC
448 content, with values >4%, results from the rise in productivity most likely due to the formation of an
449 isolated and very shallow environment (shallow lake or marsh). An organic-rich sediment succession is
450 characterized by the presence of Chara remains, implying deposition in a shallow freshwater
451 environment. The upper part of unit LU2a, with dark and light laminations, is characterized by algal
452 organic matter and the higher carbonate content (Fig. 4). This change within LU2a possibly reflects the
453 deepening of the Lošinj paleolake and variations in the main organic matter source over time. Aeolian
454 material could also contribute to the deposition in the Lošinj paleolake, as evidenced by the increase
455 in grain size (Fig. 4). Strong winds in the region during MIS 3 were assumed in the research of aeolian
456 and pedosedimentary successions conducted by Wacha et al. (2011a,b; 2017) and Mikulčić-Pavlaković
457 et al. (2011) on the nearby Island of Susak. The presence of brackish-to-freshwater macrofossil
458 assemblages throughout LU2a proves the development of a predominantly freshwater lacustrine body
459 with limited marine influence. The recognized mollusk genera (*Bithynia tentaculata*) usually inhabit
460 freshwater environments (Seddon, 2014), but they are tolerant to a wider salinity range (Carlsson,
461 2006; Cadée, 2015). The presence of foraminifera specimens that are poorly preserved could be

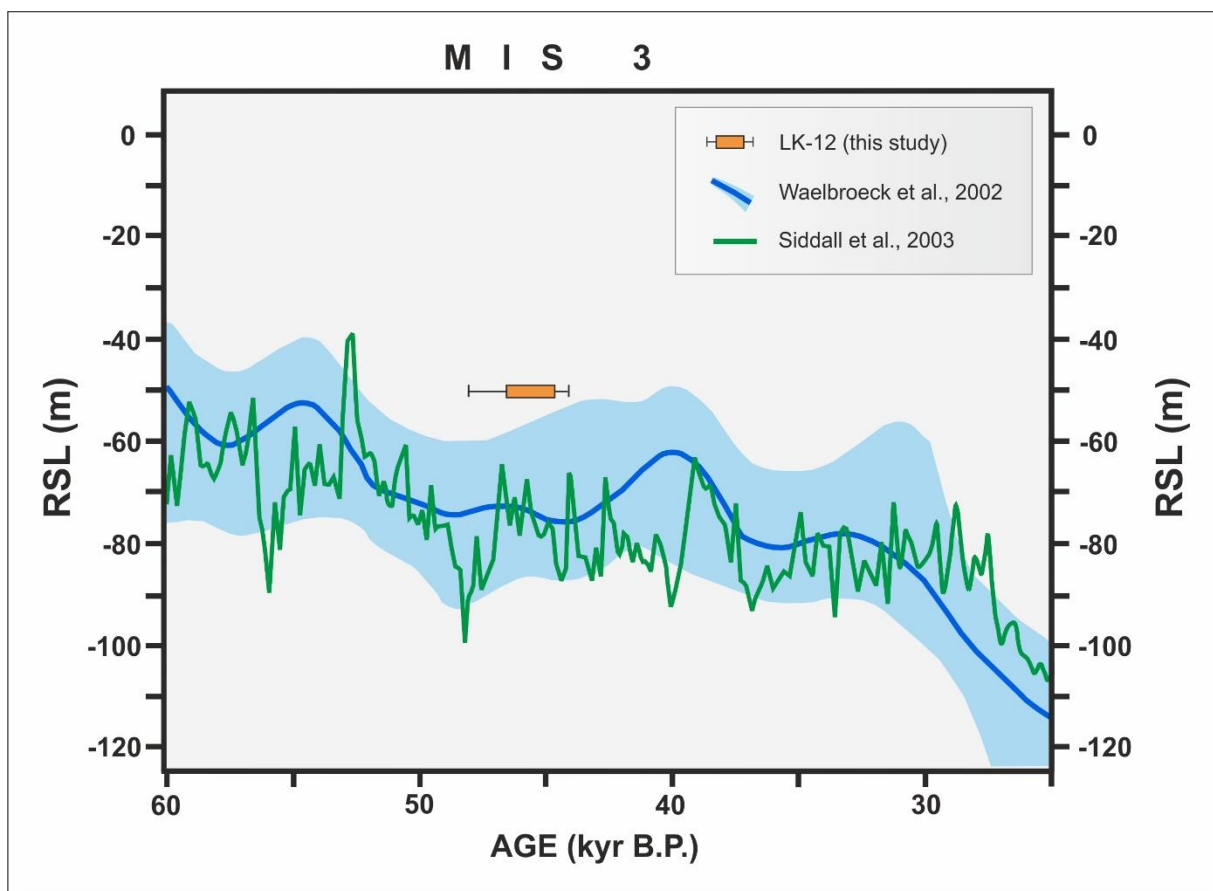
462 indicative of the establishment of unfavorable environmental conditions for their preservation, or they
463 could be reworked.

464 **5.3.2. Paleoenvironmental reconstruction considering sea level fluctuations and sill depth**

465 A sea level rise after the MIS 4 lowstand probably led to a rise in the groundwater table in the
466 investigated area and a karst lake was formed during MIS 3 (46.5 - 44.7 cal kyr B.P.) (Figs. 8C and 9C).
467 The formation of the Lošinj paleolake was probably facilitated by favorable climatic conditions in the
468 region. MIS 3 is characterized by significant variations in climate and sea level on centennial and
469 millennial time scales (Siddall et al., 2008; Rasmussen et al., 2014; Badino et al., 2019). The presence
470 of lacustrine sediments in the Lošinj basin suggests that the RSL between 46.5 - 44.7 cal kyr B.P. was
471 below the Cres sill depth of -50 m (sea level limiting point; Fig. 10). Global sea level data placed MIS 3
472 sea level at -60 to -90 m (Waelbroeck et al., 2002; Siddall et al., 2003; Siddall et al., 2008; Rohling et
473 al., 2008) (Fig. 10). Previously conducted studies in the Kvarner area also implied that MIS 3 RSL was
474 50-60 m lower than at present (Surić et al., 2014), which would have enabled marine flooding of the
475 Kvarnerić Bay through Škarda-Ist sill. Therefore, it is likely that during this time interval Kvarnerić Bay
476 was a marine environment. However, the Cres sill (-50 m) acted as a barrier, allowing the formation of
477 an isolated Lošinj paleolake (Fig. 9C). Possible seawater seepage from the Kvarnerić Bay to the Lošinj
478 paleolake, as evidenced by brackish fauna, occurred through karstified limestones in the southeastern
479 part of the investigated area where the limestone barrier is narrow. A preserved 89-cm-thick lacustrine
480 sequence proved dynamic environmental conditions in the study area during this stage. It is likely that
481 the Lošinj paleolake existed for a longer time period, but deposits were eroded or possibly never
482 deposited in the investigated part of the Lošinj basin due to the basin morphology (Fig. 2).

483 The existence of lacustrine deposits below postglacial marine deposits in karst depressions
484 along the eastern Adriatic coast has only been hypothesized and partially proved (Juračić et al., 1999;
485 Wunsam et al., 1999; Schmidt et al., 2001). This research provides clear evidence of the development
486 of a restricted, lacustrine environment with possible marine influence during MIS 3 sea level lowstand

487 (Figs. 8C and 9C). A similar paleoenvironmental evolution has been investigated in the Black Sea and
488 Marmara Sea (Çağatay et al., 2003; Bahr et al., 2005; Taviani et al., 2014; Filikci et al., 2017), where
489 lacustrine deposits preceded the Holocene marine deposition due to the existence of a sill. The
490 distinctiveness of the Lošinj paleolake is that it was formed during MIS 3 in a karstified environment.
491 Furthermore, MIS 3 lacustrine or marine deposits have not been previously reported with certainty
492 along the eastern Adriatic coast, although sedimentary records of this age have been studied along the
493 western coast of the Adriatic Sea (Amorosi et al., 2004).



494

495 Fig. 10. MIS 3 sea level limiting point from the Lošinj Channel (LK-12) plotted against global eustatic
496 sea level curve by Waelbroeck et al. (2002) (blue line) and sea level curve given by Siddall et al. (2003)
497 (green line).

498 **5.4. Karst polje phase (?44.7-13.7 cal kyr B.P.)**

499 **5.4.1. Paleoenvironmental reconstruction based on seismic and core data**

500 Seismic data revealed the existence of several phases of erosion within SU2 and between SU2
501 and SU3. These events were recognized as high amplitude unconformities (UC2, UC3 and UC4) that
502 truncate underlying reflectors (Fig. 2). Evidence of these events can also be observed in core LK-12. An
503 age-depth model provided an age of the top of lower laminated lacustrine lithological unit (LU2a) of
504 44.7 cal kyr B.P., whereas the upper brown homogenous unit (LU3) was dated at 13.7 cal kyr B.P (Fig.
505 3). This suggests the existence of a long erosional and/or depositional hiatus in LK-12 coring area.
506 However, the basal part of sediment core LK-15 (lithological unit LU2b) corresponds to the seismic
507 subunit SU2c, deposited after the development of UC3 and prior to the development of UC4 (Fig. 6
508 and Table 2). The results revealed the deposition of predominantly chaotic silty sediments, with high
509 carbonate content. It is possible that LU2b sediments are redeposited lacustrine sediments. The
510 occurrence of larger gravel-sized carbonate clasts that were most likely eroded from the surrounding
511 islands was observed. This part of the core is almost devoid of macropaleontological remains, except
512 for a few heavily fragmented gastropod shells, indicating unfavorable conditions for their preservation
513 and/or transport. Time constraints on the deposition of these sediments cannot be obtained, since
514 reliable and datable material is not present.

515 **5.4.2. Paleoenvironmental reconstruction considering sea level fluctuations and sill depth**

516 We suggest that with the substantial decrease in sea level leading to the LGM (Fairbanks, 1989;
517 Lambeck and Purcell, 2005; Lambeck et al., 2014), lacustrine deposition in the Lošinj basin ceased due
518 to the drop in the groundwater table. Therefore, favorable conditions for the formation of a karst polje
519 were established again (Figs. 8D and 9D). Periodical streams in a karst polje most likely partially eroded
520 previously deposited MIS 3 lacustrine sediments. We assume that the clasts found in basal part of LK-
521 15 core were deposited during the discharge periods. It is probable that phases of lacustrine and karst
522 polje environments exchanged in the Lošinj basin during the Last Glacial cycle in relation to the

523 oscillations in the RSL and climate, whereas in the northern Adriatic Shelf a large alluvial plain has been
524 developed (Fig. 1B) (e.g., Amorosi et al., 2003; Pellegrini et al., 2018).

525 **5.5. Marine lake phase (13.7-10.5 cal kyr B.P.)**

526 **5.5.1. Paleoenvironmental reconstruction based on seismic and core data**

527 Re-establishment of sediment accumulation in the area where sediment core LK-12 was
528 collected commenced at 13.7 cal kyr B.P. (subunits LU3a and LU3b) (Fig. 6). Sediments from these
529 lithological subunits can probably be attributed to the base of the semi-transparent seismic unit SU3,
530 deposited after UC4 erosional event (Table 2). Acoustically semi-transparent seismic unit SU3 onlaps
531 (marine onlap) onto the previously described units and acoustic basement (Fig. 2). Sediments
532 attributed to LU3 are organic-rich (TOC >2%) and predominantly silty. A gradual increase in the Sr/Ca
533 ratios implies a growing marine influence in the Lošinj basin (Fig. 6). Two distinct paleoenvironmental
534 subphases were recognized in the period from 13.7 cal kyr B.P. to 10.5 cal kyr B.P., corresponding to
535 the lithological subunits LU3a and LU3b in core LK-12 (Fig. 6).

536 High Ti/Ca ratios and MS, during the first subphase from 13.7-13.6 cal kyr B.P. (LU3a), indicate
537 significant siliciclastic terrestrial input, most likely due to the proximity of the coast to the coring
538 location. It is probable that erosion and redeposition of sediments were significant during this phase.
539 This could also suggest enhanced precipitation in the investigated area. Increase in terrestrial input
540 during Bølling-Allerød was also observed in other parts of the Adriatic Sea (Goudeau et al., 2014). The
541 contribution of algal organic matter in subunit LU3a was less important compared to terrestrially
542 derived organic matter, as evidenced by higher C/N ratios (Fig. 4). The results imply the development
543 of a shallow water environment with increased productivity. It is probable that a marsh or a shallow
544 lake was formed during this subphase. This interpretation was reinforced by mollusk assemblages that
545 are typical for freshwater-to-brackish-water conditions (*Theodoxus* sp., *Bithynia tentaculata*). In the
546 analyzed samples, shallow marine or brackish water foraminifera species *Aubignyna planidorso*,

547 *Elphidium translucens* and *Ammonia tepida* (Murray et al., 2000; Debenay and Guillou, 2002; Murray,
548 2006) were present, indicating the marine influence.

549 At 13.6 cal kyr B.P. (subunit LU3b), a marked change in sedimentation occurred. Sediments in
550 this subunit show increased CaCO₃ and TOC content, with poorly preserved laminations. The organic
551 matter is predominantly of algal source (Meyers, 1994; Meyers, 2003; Lamb et al., 2006). Terrestrial
552 input proxies (Ti/Ca, MS) account for a smaller contribution of the detrital sediment component. This
553 might indicate a phase of arid conditions in the area at 13.6 cal kyr B.P. and prior to the onset of the
554 Younger Dryas or shoreline migration and establishment of a deeper lacustrine environment. Rich
555 molluskan fauna (*Theodoxus* sp., *Bithynia tentaculata*) support the existence of brackish water
556 environmental conditions. Foraminifera specimens are well preserved and slightly more abundant
557 compared to LU3a, implying a growing marine influence. The dominant species (*Ammonia tepida* and
558 *Criboelphidium gunteri*) can dwell in brackish water environments (Debenay and Guillou, 2002;
559 Boudreau et al., 2001), and their abundances in the analyzed samples are high.

560 **5.5.2. Paleoenvironmental reconstruction considering sea level fluctuations and sill depth**

561 We propose that the formation of shallow and eventually deeper brackish water lacustrine
562 environment (marine lake) in the Lošinj karst basin, occurred with the rapidly rising sea level during
563 the Allerød interstadial, at 13.7 cal kyr B.P. The onset of the abrupt post-LGM sea level rise (Waelbroek
564 et al., 2002; Lambeck et al., 2014) led to the rise in the groundwater table in the investigated area. The
565 data obtained in this study suggest that RSL in the Lošinj Channel during the Allerød was <-50 m. It is
566 considered that during the Allerød interstadial, the global sea level was approximately -75 to -60 m
567 lower than at present (Waelbroeck et al., 2002; Lambeck et al., 2014). It is probable that during this
568 time period Kvarnerić Bay was a marine environment (Fig. 9E). However, the Cres sill was again a
569 barrier that isolated the Lošinj marine lake from the direct marine influence from the Kvarnerić Bay
570 (Figs. 8E and 9E). The formation of marine lake was aided by strong diffusion of seawater through
571 karstified Cres sill from the Kvarnerić Bay and high precipitation. Similar environments have been

572 recognized along the present-day eastern Adriatic coast (e.g., Mljet Lakes, Lake Mir, Zmajevsko oko)
573 (Surić, 2002; Surić, 2005; Pikelj and Juračić, 2013).

574 Although the Allerød sediment sequence in the Lošinj basin is well preserved, Schmidt et al.
575 (2000) have postulated that a gap in sedimentation occurred during the Allerød interstadial in the
576 nearby Lake Vrana on the Island of Cres. In the same time frame, the paleoenvironmental evolution of
577 the northern Adriatic shelf was significantly different, with alluvial channels and plains developed
578 during the LGM exhibiting retrogradational patterns (e.g., Amorosi et al., 2003; Correggiari et al., 2005;
579 Moscon et al., 2015; Benjamin et al., 2017).

580 **5.6. Marine phase (10.5 cal kyr B.P.-present)**

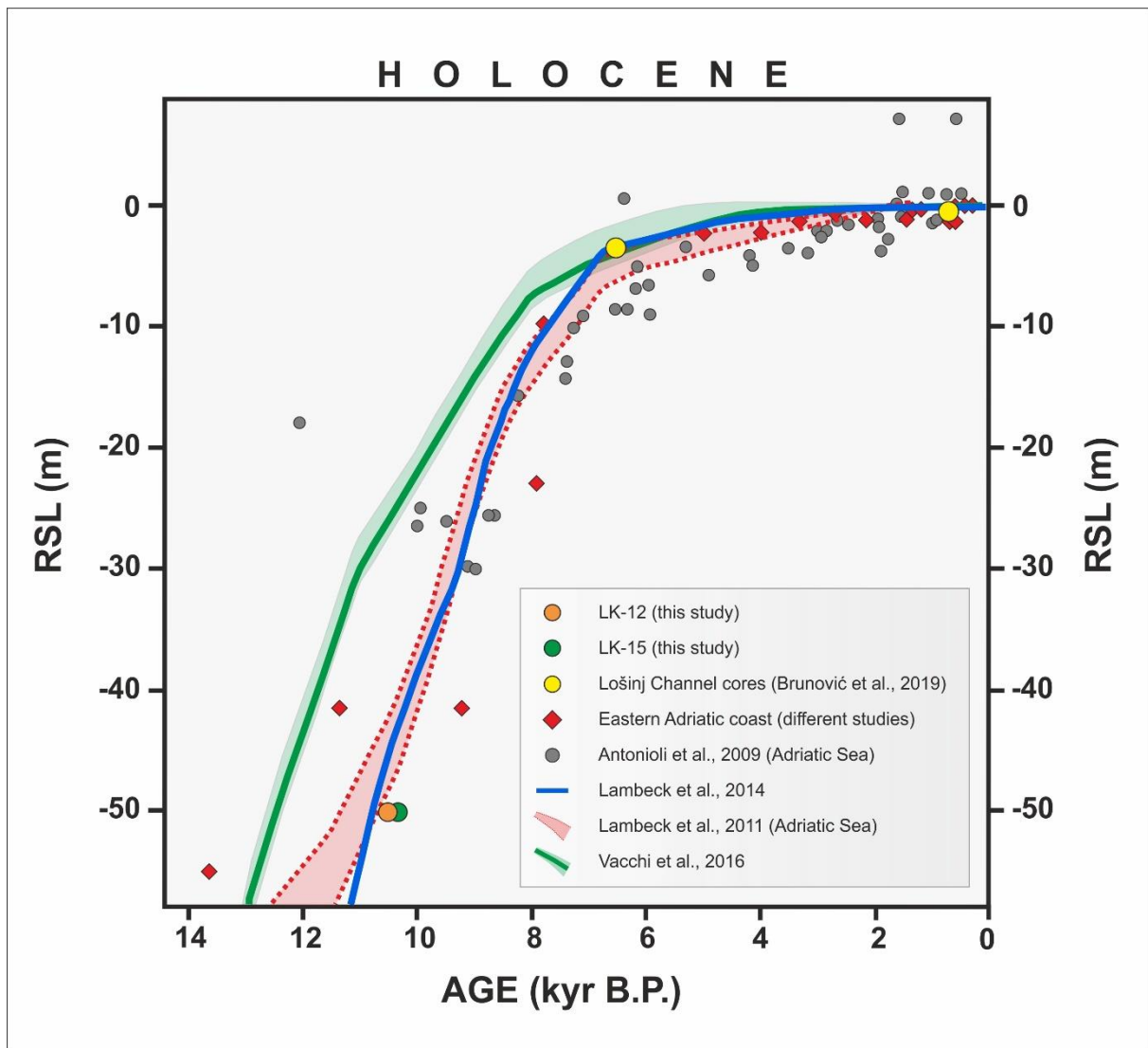
581 **5.6.1. Paleoenvironmental reconstruction based on seismic and core data**

582 An environmental phase during which the Lošinj marine lake was a restricted environment,
583 without surface connection to the sea on the other side of the Cres sill, existed for approximately 3000
584 years. At 10.5 cal kyr B.P., a noticeable shift can be observed in the multi-proxy data from sediment
585 core LK-12 (unit LU4) (Fig. 6). In sediment core LK-15 this transition was dated at 10.3 cal kyr B.P.
586 Seismic data (SU3) also indicated the deposition of sediments with different lithologic properties (Fig.
587 2 and Table 2). The Sr/Ca ratio abruptly increased (Fig. 6), implying marine flooding of the Lošinj karst
588 basin (Figs. 8F and 9F). The Holocene marine sedimentary succession is characterized by a coarser
589 grain-size, low productivity, terrestrial organic matter input and a rise in terrigenous siliciclastic input
590 (high MS, Ti/Ca) (Fig. 4). This rise is likely related to the onset of a pluvial period with intensified soil
591 erosion from the catchment. The Holocene pluvial period has been previously described in the Adriatic
592 Sea (Wunsam et al., 1999; Schmidt et al., 2000; Schmidt et al., 2001; Combourieu-Nebout et al., 2013).
593 The topmost part of the core LK-12 (from 37 cm upcore) is characterized by decreases in MS and Ti/Ca
594 ratios at 5.8 cal kyr B.P., which could mark the end of the humid climate conditions. This is in general
595 accordance with the previously published data (Wunsam et al., 1999; Schmidt et al., 2001;
596 Combourieu-Nebout et al., 2013). Paleontological analysis provided strong evidence of surface

597 connectivity with the Kvarnerić Bay (Fig. 6). Typical marine mollusks appear (*Mytilus* sp., *Cerastoderma*
598 sp.), and foraminifera specimens become significantly more abundant and diversified compared to the
599 previous phase. Assemblages are dominated by *Elphidium translucens*, *Epistominella exuiga*,
600 *Asterigerinata adriatica* and *Textularia conica*. The recognized Holocene assemblage is similar to
601 assemblages described in greater water depth and high productivity environments along the eastern
602 Adriatic coast (Vidović, 2010).

603 **5.6.2. Paleoenvironmental reconstruction considering sea level fluctuations and sill depth**

604 Based on the two analyzed sediment cores, we have determined with confidence that sea level
605 reached the Cres sill depth of -50 m during the Holocene, in the period between 10.5-10.3 cal kyr B.P.
606 At that time RSL was high enough for marine sedimentation to occur and Cres sill no longer had a
607 function of a barrier (Figs. 8F and 9F). Many papers assessed the Holocene RSL changes in the Adriatic
608 (e.g., Lambeck et al., 2004, 2011; Antonioli et al., 2009; Faivre et al., 2011, 2013; Vacchi et al., 2016;
609 Shaw et al., 2016, 2018). However, most of the observational data are of Late Holocene age and were
610 collected along the western coast of the Adriatic Sea. In Fig. 11 we compared our RSL data with the
611 already published observational RSL evidence from the region (Malez et al., 1979; Wunsam et al., 1999;
612 Govorčin et al., 2001; Schmidt et al., 2001; Surić et al., 2004; Antonioli et al., 2009; Surić and Juračić,
613 2010; Faivre et al., 2013; Brunović et al., 2019), predicted RSL obtained using the models published for
614 the Adriatic Sea and Mediterranean (Lambeck et al., 2011, Vacchi et al., 2016), and eustatic sea level
615 changes (Lambeck et al., 2014). We highlight the possibility that the Lošinj basin data suggest a tectonic
616 subsidence of the area during the Holocene, considering that the observed data lie below the predicted
617 and eustatic values. The Holocene subsidence trends along the eastern Adriatic coast have been
618 previously reported by Antonioli et al. (2009), Faivre et al. (2011; 2019) and Shaw et al. (2018).
619 However, we also do not dismiss the possibility that the Lošinj basin was flooded with seawater before
620 10.5 cal kyr B.P when marine sedimentation started. Therefore, the obtained data are sea level limiting
621 points.



622
 623 Fig. 11. The Holocene RSL observations from this study (LK-12 and LK-15), Adriatic Sea (Antonioli et al.,
 624 2009) and eastern Adriatic coast (Malez et al., 1979; Wunsam et al., 1999; Govorčin et al., 2001;
 625 Schmidt et al., 2001; Surić et al., 2005; Surić and Juračić, 2010; Faivre et al., 2013) plotted against
 626 eustatic sea level curve by Lambeck et al., 2014 (blue line), and regional RSL models by Lambeck et al.
 627 (2011) (red line) and Vacchi et al. (2016) (green line). Previously published sea level data from the
 628 Lošinj Channel are also plotted on the graph (Brunović et al., 2019).

629 **6. Conclusions**

630 This research provided an insight into the long-term Late Pleistocene and Holocene
631 paleoenvironmental development of the Lošinj Channel. A crucial factor for preservation of the thick
632 Quaternary sediment succession is the geomorphological setting of the eastern Adriatic coast. Silled
633 karst basins, such as the Lošinj Channel, act as a trap for sediments and therefore contain long records
634 of paleoenvironmental changes. These changes were driven by substantial sea level and climate
635 variations that occurred during the Quaternary glacial-interglacial transitions.

636 Extracted sediment cores LK-12 and LK-15 and seismic reflection profile revealed a complex
637 suite of very different depositional environments in the Lošinj karst basin. The combined use of
638 geochemical, sedimentological, and paleontological proxies combined with radiocarbon dating are
639 shown to be valuable indicators for the interpretation of past environments in these settings. Our
640 results include a presumed MIS 5a marine sediment succession deposited when the RSL was higher
641 than -50 m Cres sill depth. An important feature is the development of a brackish-to-freshwater Lošinj
642 paleolake during MIS 3. This is significant since it suggests the presence of an isolated lacustrine karst
643 basin along the eastern Adriatic coast. The sea level drop that followed was characterized by the
644 formation of a karst polje, with the probable occurrence of periodic streams. The post-LGM period was
645 marked by re-establishment of the deposition in a brackish water marine lake. The RSL reached a depth
646 of -50 m at 10.5 cal kyr B.P., which led to a marine flooding of the Lošinj Channel. The obtained data
647 are important for the reconstruction of RSL and climate variations along the eastern Adriatic coast.
648 Furthermore, the investigated submerged karst basin enhances our understanding of
649 paleoenvironmental development in karstified systems and implies the formation of brackish water
650 conditions prior to the actual flooding of the basin due to the rising sea level.

651 Further importance of our study stems from the fact that only 15 cores included in the
652 Mediterranean sediment core database published by Alberico et al. (2017) penetrated the Younger
653 Dryas boundary. Therefore, the Lošinj Channel data are also significant on a wider regional scale.

654 Although this research provided many new observations, some questions still remain
655 unanswered. The age of older marine succession and possible variations in the depth of the Cres sill in
656 relation to the vertical tectonic movements and glacio-hydro-isostatic adjustment should be
657 investigated in the future. We can also assume that there is a cyclicity in the development of
658 depositional environments in the deep silled karst depressions, which even further stresses the
659 importance of the eastern Adriatic coast for Quaternary research.

660 **Acknowledgments**

661 This research was performed within the project „Lost Lake Landscapes of the Eastern Adriatic
662 Shelf“ (LoLADRIA; project no. 9419), supported by the Croatian Science Foundation (HRZZ). The
663 authors would like to thank Nikos Georgiou, Xenophon Dimas, Spyros Sergiou, Dimitris Christodoulou,
664 George Ferentinos and Margarita Iatrou from the University of Patras for their support during the
665 seismic survey and during the interpretation of the seismic data. We are also thankful to Ivan Razum,
666 Hrvoje Burić and Edin Badnjević for their help during the coring campaign and Ana-Maria Heski and
667 Martina Šparica-Miko for laboratory analyses. This paper is partly the result of training and education
668 conducted through GeoTwinn project that has received funding from the European Union’s Horizon
669 2020 research and innovation programme under grant agreement no. 809943. We would like to thank
670 two anonymous reviewers for their time and effort in reading the manuscript and making valuable
671 notes for its improvement.

672 **References**

- 673 Aksu, A.E., Hiscott, R.N., Mudie, P.J., Rochon, A., Kaminski, M.A., Abrajano, T., Yaşar, D., 2002.
674 Persistent Holocene Outflow from the Black Sea to the Eastern Mediterranean Contradicts
675 Noah's Flood Hypothesis. *GSA Today* 12, 4-9.
- 676 Alberico, I., Giliberti, I., Insinga, D.D., Petrosino, P., Vallefucoco, M., Lirer, F., Bonomo, S., Cascella, A.,
677 Anzalone, E., Barra, R., Marsella, E., Ferraro, L., 2017. Marine sediment cores database for the

678 Mediterranean Basin: A tool for past climatic and environmental studies. *Open Geosci.* 9, 221–
679 239. <https://doi.org/10.1515/geo-2017-0019>

680 Amorosi, A., Centineo, M.C., Colalongo, M.L., Pasini, G., Sarti, G., Vaiani, S.C., 2003. Facies Architecture
681 and Latest Pleistocene–Holocene Depositional History of the Po Delta (Comacchio Area), Italy.
682 *J. Geol.* 111, 39–56. <https://doi.org/10.1086/344577>

683 Amorosi, A., Colalongo, M.L., Fiorini, F., Fusco, F., Pasini, G., Vaiani, S.C., Sarti, G., 2004.
684 Palaeogeographic and palaeoclimatic evolution of the Po Plain from 150-ky core records. *Glob.*
685 *Planet. Change* 40, 55–78. [https://doi.org/10.1016/S0921-8181\(03\)00098-5](https://doi.org/10.1016/S0921-8181(03)00098-5)

686 Amorosi, A., Fontana, A., Antonioli, F., Primon, S., Bondesan, A., 2008. Post-LGM sedimentation and
687 Holocene shoreline evolution in the NW Adriatic coastal area. *GeoActa* 7, 41–67.

688 Antonioli, F., Ferranti, L., Fontana, A., Amorosi, A., Bondesan, A., Braitenberg, C., Dutton, A., Fontolan,
689 G., Furlani, S., Lambeck, K., Mastronuzzi, G., Monaco, C., Spada, G., Stocchi, P., 2009. Holocene
690 relative sea-level changes and vertical movements along the Italian and Istrian coastlines.
691 *Quat. Int.* 206, 102–133. <https://doi.org/10.1016/j.quaint.2008.11.008>

692 Antonioli, F., Anzidei, M., Amorosi, A., Lo Presti, V., Mastronuzzi, G., Deiana, G., De Falco, G., Fontana,
693 A., Fontolan, G., Lisco, S., Marsico, A., Moretti, M., Orrù, P.E., Sannino, G.M., Serpelloni, E.,
694 Vecchio, A., 2017. Sea-level rise and potential drowning of the Italian coastal plains: Flooding
695 risk scenarios for 2100. *Quat. Sci. Rev.* 158, 29–43.
696 <https://doi.org/10.1016/j.quascirev.2016.12.021>

697 Babić, L., Crnjaković, M., Asmerom, Y., 2012. Uplifted Pleistocene marine sediments of the Central
698 Adriatic Island of Brusnik. *Geol. Croat.* 65, 223–232. <https://doi.org/10.4154/gc.2012.13>

699 Badino, F., Pini, R., Ravazzi, C., Margaritora, D., Arrighi, S., Bortolini, E., Figus, C., Giaccio, B., Lugli, F.,
700 Marciani, G., Monegato, G., Moroni, A., Negrino, F., Oxilia, G., Peresani, M., Romandini, M.,

701 Ronchitelli, A., Spinapolice, E.E., Zerboni, A., Benazzi, S., 2019. An overview of Alpine and
702 Mediterranean palaeogeography, terrestrial ecosystems and climate history during MIS 3 with
703 focus on the Middle to Upper Palaeolithic transition. *Quat. Int.* 1–22.
704 <https://doi.org/10.1016/j.quaint.2019.09.024>

705 Bahr, A., Lamy, F., Arz, H., Kuhlmann, H., Wefer, G., 2005. Late glacial to Holocene climate and
706 sedimentation history in the NW Black Sea. *Mar. Geol.* 214, 309–322.
707 <https://doi.org/10.1016/j.margeo.2004.11.013>

708 Bailey, G.N., Flemming, N.C., 2008. Archaeology of the continental shelf: Marine resources, submerged
709 landscapes and underwater archaeology. *Quat. Sci. Rev.* 27, 2153–2165.
710 <https://doi.org/10.1016/j.quascirev.2008.08.012>

711 Balascio, N.L., Zhang, Z., Bradley, R.S., Perren, B., Dahl, S.O., Bakke, J., 2011. A multi-proxy approach to
712 assessing isolation basin stratigraphy from the Lofoten Islands, Norway. *Quat. Res.* 75, 288–
713 300. <https://doi.org/10.1016/j.yqres.2010.08.012>

714 Becker, J. J., Sandwell, D. T., Smith, W. H. F., Braud, J., Binder, B., Depner, J., Fabre, D., Factor, J., Ingalls,
715 S., Kim, S.H., Ladner, R., Marks, K., Nelson, S., Pharaoh, A., Sharman, G., Trimmer, R.,
716 VonRosenburg, J., Wallace, G., Weatherall, P., 2009. Global Bathymetry and Elevation Data at
717 30 Arc Seconds Resolution: SRTM30_PLUS. *Marine Geodesy* 32/4, 355-371.

718 Benjamin, J., Rovere, A., Fontana, A., Furlani, S., Vacchi, M., Inglis, R.H., Galili, E., Antonioli, F., Sivan,
719 D., Miko, S., Mourtzas, N., Felja, I., Meredith-Williams, M., Goodman-Tchernov, B., Kolaiti, E.,
720 Anzidei, M., Gehrels, R., 2017. Late Quaternary sea-level changes and early human societies in
721 the central and eastern Mediterranean Basin: An interdisciplinary review. *Quat. Int.* 449, 29–
722 57. <https://doi.org/10.1016/j.quaint.2017.06.025>

723 Blaauw, M., 2010. Methods and code for „classical“ age-modelling of radiocarbon sequences.
724 *Quaternary Geochronology* 5, 512-518.

725 Blanchet, C.L., Tjallingii, R., Frank, M., Lorenzen, J., Reitz, A., Brown, K., Feseker, T., Brückmann, W.,
726 2013. High- and low-latitude forcing of the Nile River regime during the Holocene inferred from
727 laminated sediments of the Nile deep-sea fan. *Earth Planet. Sci. Lett.* 364, 98–110.
728 <https://doi.org/10.1016/j.epsl.2013.01.009>

729 Blott, S.J., Pye, K., 2001. Gradstat: A Grain Size Distribution and Statistics Package for the Analysis of
730 Unconsolidated Sediments. *Earth Surf. Process. Landforms* 26, 1237–1248.
731 <https://doi.org/10.1002/esp.261>

732 Bonacci, O., 2013. Poljes, Ponders and Their Catchments, in: Frumkin, A. (Eds.), *New Developments of*
733 *Karst Geomorphology Concepts, Treatise on Geomorphology*, pp. 112-119
734 <https://doi.org/10.1016/B978-0-12-374739-6.00112-3>

735 Boudreau, R.E.A., Patterson, T.R., Dalby, A.P., McKillop, B.W., 2001. Non-marine occurrence of the
736 foraminifer *Cibicides lobatulus* in northern Lake Winnipegosis, Manitoba, Canada. *J. Foraminif. Res.* 29, 108–119. <https://doi.org/10.2113/0310108>

738 Brunović, D., Miko, S., Ilijanić, N., Peh, Z., Hasan, O., Kolar, T., Šparica Miko, M., Razum, I., 2019.
739 Holocene environmental evolution recorded in the coastal karst dolines on the Island of Cres,
740 Croatia. *Geologia Croatica* 72/1, 19-42

741 Cadée, G.C., 2015. Shell repair in the freshwater gastropod *Bithynia tentaculata* (Linnaeus, 1758). *Vita*
742 *Malacologica* 13, 31–34.

743 Çağatay, M.N., Görür, N., Polonia, A., Demirbağ, E., Sakiñç, M., Cormier, M.H., Capotondi, L., McHugh,
744 C., Emre, Ö., Eriş, K., 2003. Sea-level changes and depositional environments in the İzmit Gulf,
745 eastern Marmara Sea, during the late glacial-Holocene period. *Mar. Geol.* 202, 159–173.
746 [https://doi.org/10.1016/S0025-3227\(03\)00259-7](https://doi.org/10.1016/S0025-3227(03)00259-7)

747 Çağatay, M.N., Eriş, K.K., Makaroğlu, Ö., Yakupoğlu, N., Henry, P., Leroy, S.A.G., Uçarkuş, G., Sakıncı, M.,
748 Yalamaz, B., Bozyiğit, C., Kende, J., 2019. The Sea of Marmara during Marine Isotope Stages 5
749 and 6. *Quat. Sci. Rev.* 220, 124–141. <https://doi.org/10.1016/j.quascirev.2019.07.031>

750 Campo, B., Amorosi, A., Vaiani, S.C., 2017. Sequence stratigraphy and late Quaternary
751 paleoenvironmental evolution of the Northern Adriatic coastal plain (Italy). *Palaeogeogr.*
752 *Palaeoclimatol. Palaeoecol.* 466, 265–278. <https://doi.org/10.1016/j.palaeo.2016.11.016>

753 Carlsson, R., 2006. Freshwater snail assemblages of semi-isolated brackish water bays on the Åland
754 Islands, SW Finland. *Boreal Environ. Res.* 11, 371–382.

755 Caruso, A., Cosentino, C., Pierre, C., Sulli, A., 2011. Sea-level changes during the last 41,000 years in
756 the outer shelf of the southern Tyrrhenian Sea: Evidence from benthic foraminifera and
757 seismostratigraphic analysis. *Quaternary International* 232(1–2), 122–131.
758 <https://doi.org/10.1016/j.quaint.2010.07.034>.

759 Cimerman, F., Langer, M.R., 1991. Mediterranean foraminifera. *Razred za naravoslovne vede, classis*
760 *IV: historia naturalis, opera* 30. Slovenska Akademija, Ljubljana.

761 Combourieu-Nebout, N., Peyron, O., Bout-Roumazielles, V., Goring, S., Dormoy, I., Joannin, S., Sadori,
762 L., Siani, G., Magny, M., 2013. Holocene vegetation and climate changes in the central
763 Mediterranean inferred from a high-resolution marine pollen record (Adriatic Sea). *Clim. Past*
764 9, 2023–2042. <https://doi.org/10.5194/cp-9-2023-2013>

765 Correggiari, A., Roveri, M., Trincardi, F., 1996. Late Pleistocene and Holocene Evolution of the North
766 Adriatic Sea. *Il Quaternario* 9, 697-704.

767 Correggiari, A., Trincardi, F., Langone, L., Roveri, M., 2001. Styles of failure in late Holocene highstand
768 prodelta wedges on the Adriatic shelf. *J. Sediment. Res.* 71, 218–236.
769 <https://doi.org/10.1306/042800710218>

- 770 Correggiari, A., Cattaneo, A., Trincardi, F., 2005. The modern Po Delta system: Lobe switching and
771 asymmetric prodelta growth. *Marine Geology* 222-223, 49-74.
- 772 Cosentino, C., Molisso, F., Scopelliti, G., Caruso, A., Insinga, D.D., Lubritto, C., Pepe, F., Sacchi, M., 2017.
773 Benthic foraminifera as indicators of relative sea-level fluctuations: Paleoenvironmental and
774 paleoclimatic reconstruction of a Holocene marine succession (Calabria, south-eastern
775 Tyrrhenian Sea). *Quat. Int.* 439, 79–101. <https://doi.org/10.1016/j.quaint.2016.10.012>
- 776 Croudace, I.W., Rindby, A., Rothwell, R.G., 2006. ITRAX: description and evaluation of a new multi-
777 function X-ray core scanner. *Geol. Soc. London, Spec. Publ.* 267, 51–63.
778 <https://doi.org/10.1144/GSL.SP.2006.267.01.04>
- 779 Croudace, I.W., Rothwell, R.G., 2015. *Micro-XRF Studies of Sediment Cores: Applications of a non-
780 destructive tool for the environmental sciences (Developments in Paleoenvironmental
781 Research), Tracking Environmental Change Using Lake Sediments. Volume 2: Physical and
782 Geochemical Methods.* Springer, Dordrecht. <https://doi.org/10.1007/978-94-017-9849-5>
- 783 Debenay, J.P., Guillou, J.J., 2002. Ecological transitions indicated by foraminiferal assemblages in
784 paralic environments. *Estuaries* 25, 1107–1120. <https://doi.org/10.1007/BF02692208>
- 785 Dorale, J.A., Onac, B.P., Fornós, J.J., Ginés, J., Ginés, A., Tuccimei, P., Peate, D.W., 2010. Sea-level
786 highstand 81, 000 years ago in mallorca. *Science* 327, 860–863.
787 <https://doi.org/10.1126/science.1181725>
- 788 Fairbanks, R.G., 1989. A 17.000-yr glacio-eustatic sea level record: influence of glacial melting rates on
789 the Younger Dryas event and deep-ocean circulation. *Nature* 342, 637-642.
- 790 Faivre, S., Bakran-Petricioli, T., Barešić, J., Horvatinčić, N., 2015. New Data On Marine Radiocarbon
791 Reservoir Effect In The Eastern Adriatic Based On Pre-Bomb Marine Organisms From The

792 Intertidal Zone And Shallow Sea. Radiocarbon 57, 527-538.
793 https://doi.org/10.2458/azu_rc.57.18452

794 Faivre, S., Bakran-Petricioli, T., Horvatinčić, N., Sironić, A., 2013. Distinct phases of relative sea level
795 changes in the central Adriatic during the last 1500 years-influence of climatic variations?
796 *Palaeogeography, Palaeoclimatology, Palaeoecology* 369, 163-174.

797 Faivre, S., Fouache, E., Ghilardi, M., Antonioli, F., Furlani, S., Kovačić, V., 2011. Relative sea level change
798 in western Istria (Croatia) during the last millennium. *Quat. Int.* 232, 132–143.
799 <https://doi.org/10.1016/j.quaint.2010.05.027>

800 Faivre S., Bakran-Petricioli, T., Barešić, J., Horvatić, D., Macario, R., 2019. Relative sea-level change and
801 climate change in the Northeastern Adriatic during the last 1.5 ka (Istria, Croatia). *Quat. Sci.*
802 *Rev.* 222. <https://doi.org/10.1016/j.quascirev.2019.105909>

803 Fedje, D., McLaren, D., James, T.S., Mackie, Q., Smith, N.F., Southon, J.R., Mackie, A.P., 2018. A revised
804 sea level history for the northern Strait of Georgia, British Columbia, Canada. *Quat. Sci. Rev.*
805 192, 300–316. <https://doi.org/10.1016/j.quascirev.2018.05.018>

806 Felja, I., Fontana, A., Furlani, S., Bajraktarević, Z., Paradžik, A., Topalović, E., Rossato, S., Čosović, V.,
807 Juračić, M., 2015. Environmental changes in the lower Mirna river valley (Istria, Croatia) during
808 the middle and late Holocene. *Geol. Croat.* 68. <https://doi.org/10.4154/gc.2015.16>

809 Filikci, B., Eriş, K.K., Çağatay, N., Sabuncu, A., Polonia, A., 2017. Late glacial to Holocene water level and
810 climate changes in the Gulf of Gemlik, Sea of Marmara: evidence from multi-proxy data. *Geo-*
811 *Marine Lett.* 37, 501–513. <https://doi.org/10.1007/s00367-017-0498-2>

812 Flemming, N., Harff, J., Moura, D., Burgess, A., Bailey, G.N., 2017. *Submerged Landscapes of the*
813 *European Continental Shelf: Quaternary Paleoenvironments.* Wiley-Blackwell, Chichester.

- 814 Foglini, F., Prampolini, M., Micallef, A., Angeletti, L., Vandelli, V., Deidun, A., Soldati, M., Taviani, M.,
815 2015. Late Quaternary coastal landscape morphology and evolution of the Maltese Islands
816 (Mediterranean Sea) reconstructed from high-resolution seafloor data. *Geol. Soc. London,*
817 *Spec. Publ.* 411, 77–95. <https://doi.org/10.1144/SP411.12>
- 818 Folk, R.L., Ward, W.C., 1957. Brazos River bar: a study in the significance of grain size parameters. *J.*
819 *Sediment. Petrol.* 27, 3-26.
- 820 Ford, D.C., Williams, P., 2007. *Karst Hydrogeology and Geomorphology*, Wiley, London, pp. 562.
- 821 Frignani, M., Langone, L., Ravaioli, M., Sorgente, D., Alvisi, F., Albertazzi, S., 2005. Fine sediment mass
822 balance in the western Adriatic continental shelf over a century time scale. *Mar. Geol.* 222–
823 223, 113-133.
- 824 Fuček, L., Matičec, D., Vlahović, I., Oštrić, N., Prtoljan, B., Korbar, T., Husinec, A., 2012. Osnovna
825 geološka karta Republike Hrvatske mjerila 1:50 000 – list Cres 2. (Basic Geological Map of
826 Republic of Croatia 1:50 000, Cres 2 Sheet). Hrvatski geološki institut, Zagreb.
- 827 Fuček, L., Matičec, D., Vlahović, I., Oštrić, N., Prtoljan, B., Korbar, T., Husinec, A., Palenik, D., 2014.
828 Osnovna geološka karta Republike Hrvatske mjerila 1:50 000 – list Cres 4. (Basic Geological
829 Map of Republic of Croatia 1:50 000, Cres 4 Sheet). Hrvatski geološki institut, Zagreb.
- 830 Galassi, P., Marocco, R., (1999). Relative sea-level rise, sedi- ment accumulation and subsidence in the
831 Caorle Lagoon (Northern Adriatic Sea, Italy) during the Holocene. *Il Quaternario* 12, 249-256.
- 832 Geraga, M., Papatheodorou, G., Agouridis, C., Kaberi, H., Iatrou, M., Christodoulou, D., Fakiris, E.,
833 Prevenios, M., Kordella, S., Ferentinos, G., 2017. Palaeoenvironmental implications of a marine
834 geoarchaeological survey conducted in the SW Argosaronic gulf, Greece. *J. Archaeol. Sci.*
835 *Reports* 12, 805–818. <https://doi.org/10.1016/j.jasrep.2016.08.004>

836 Goudeau, M.L.S., Grauel, A.L., Tessarolo, C., Leider, A., Chen, L., Bernasconi, S.M., Versteegh, G.J.M.,
837 Zonneveld, K.A.F., Boer, W., Alonso-Hernandez, C.M., De Lange, G.J., 2014. The Glacial-
838 Interglacial transition and Holocene environmental changes in sediments from the Gulf of
839 Taranto, central Mediterranean. *Mar. Geol.* 348, 88–102.
840 <https://doi.org/10.1016/j.margeo.2013.12.003>

841 Govorčin, D.P., Juračić, M., Horvatinčić, N., Onofori, V., 2001. Holocene sedimentation in the Soline
842 Channel (Mljet Lakes, Adriatic Sea), *Natura Croatica* 10/4, 247-258.

843 Haenssler, E., Unkel, I., Dörfler, W., Nadeau, M., 2014. Driving mechanisms of Holocene lagoon
844 development and barrier accretion in Northern Elis, Peloponnese, inferred from the
845 sedimentary record of the Kotychi Lagoon. *Quat. Sci. J.* 63, 60–77.
846 <https://doi.org/10.3285/eg.63.1.04>

847 Hajek-Tadesse, V., Ilijanić, N., Miko, S., Hasan, O., 2018. Holocene Ostracoda (Crustacea) from the
848 shallow Lake Vrana (Dalmatia, Croatia) and their paleoenvironmental significance. *Quat. Int.*
849 <https://doi.org/10.1016/j.quaint.2018.01.007>

850 Ilijanić, N., Miko, S., Hasan, O., Bakrač, K., 2018. Holocene environmental record from lake sediments
851 in the Bokanjačko blato karst polje (Dalmatia, Croatia). *Quat. Int.*
852 <https://doi.org/10.1016/j.quaint.2018.01.037>

853 Juračić, M., Benac, Č., Crmarić, R., 1999. Seabed and Surface Sediment Map of the Kvamer Region,
854 Adriatic Sea, Croatia (Lithological Map, 1:500,000). *Geol. Croat.* 52, 131–140.

855 Kelletat, D.H., 2005. Dalmatian coasts, in: Schwartz, M. (Eds.), *Encyclopedia of Coastal Science.*
856 *Encyclopedia of Earth Sciences Series.* Dordrecht, The Netherlands: Springer, pp. 355–356.

857 Kent, D. V., Rio, D., Massari, F., Kukla, G., Lanci, L., 2002. Emergence of Venice during the Pleistocene.
858 *Quat. Sci. Rev.* 21, 1719–1727. [https://doi.org/10.1016/S0277-3791\(01\)00153-6](https://doi.org/10.1016/S0277-3791(01)00153-6)

859 Korbar, T., 2009. Orogenic evolution of the External Dinarides in the NE Adriatic region: a model
860 constrained by tectonostratigraphy of Upper Cretaceous to Palaeogene carbonates. *Earth-Sci.*
861 *Rev.* 96 (4), 296–312. <http://dx.doi.org/10.1016/j.earscirev.2009.07.004>.

862 Korbar, T., Fuček, L., Husinec, A., Vlahović, I., Oštrić, N., Matičec, D., Jelaska, V., 2001. Cenomanian
863 carbonate facies and rudists along shallow intraplateau basin margin—the island of Cres
864 (Adriatic Sea, Croatia). *Facies* 45, 39–58. <https://doi.org/10.1007/BF02668104>

865 Korbar, T., Husinec, A., 2003. Biostratigraphy of Turonian to (?) Coniacian Platform Carbonates : A Case
866 Study from the Island of Cres (Northern Adriatic , Croatia). *Geol. Croat.* 56, 173–186.

867 Kranjc, A., 2013. Classification of Closed Depressions in Carbonate Karst, in: Frumkin, A. (Eds.), *New*
868 *Developments of Karst Geomorphology Concepts, Treatise on Geomorphology*, pp. 104-110
869 <https://doi.org/10.1016/B978-0-12-374739-6.00112-3>

870 Lamb, A.L., Wilson, G.P., Leng, M.J., 2006. A review of coastal palaeoclimate and relative sea-level
871 reconstructions using $\delta^{13}\text{C}$ and C/N ratios in organic material. *Earth-Science Rev.* 75, 29–57.
872 <https://doi.org/10.1016/j.earscirev.2005.10.003>

873 Lambeck, K., Antonioli, F., Anzidei, M., Ferranti, L., Leoni, G., Scicchitano, G., Silenzi, S., 2011. Sea level
874 change along the Italian coast during the Holocene and projections for the future. *Quat. Int.*
875 232, 250–257. <https://doi.org/10.1016/j.quaint.2010.04.026>

876 Lambeck, K., Antonioli, F., Purcell, A., Silenzi, S., 2004. Sea-level change along the Italian coast for the
877 past 10,000 yr. *Quat. Sci. Rev.* 23, 1567–1598.
878 <https://doi.org/10.1016/j.quascirev.2004.02.009>

879 Lambeck, K., Antonioli, F., Anzidei, M., Ferranti, L., Leoni, G., Scicchitano, G., Silenzi, S., 2011. Sea level
880 change along the Italian coast during the Holocene and projections for the future. *Quat. Int.*
881 232, 250-257.

- 882 Lambeck, K., Chappell, J., 2001. Sea level change through the last glacial cycle. *Science* 292, 679–686.
883 <https://doi.org/10.1126/science.1059549>
- 884 Lambeck, K., Rouby, H., Purcell, A., Sun, Y., Sambridge, M., 2014. Sea level and global ice volumes from
885 the Last Glacial Maximum to the Holocene. *Proc. Natl. Acad. Sci.* 111, 15296–15303.
886 <https://doi.org/10.1073/pnas.1411762111>
- 887 Lambeck, K., Purcell, A., 2005. Sea-level change in the Mediterranean Sea since the LGM: model
888 predictions for tectonically stable areas. *Quaternary Science Reviews* 24, 1969–1988.
- 889 Lloyd, J.M., Evans, J.R., 2002. Contemporary and fossil foraminifera from isolation basins in northwest
890 Scotland. *J. Quat. Sci.* 17, 431–443. <https://doi.org/10.1002/jqs.719>
- 891 Lloyd, J., 2000. Combined Foraminiferal and Thecamoebian Environmental Reconstruction From an
892 Isolation Basin in NW Scotland: Implications for Sea-Level Studies. *J. Foraminifer. Res.* 30, 294–
893 305. <https://doi.org/10.2113/0300294>
- 894 Loeblich, A.R., Tappan, H., 1987. *Foraminiferal Genera and Their Classification*. Van Nostrand Reinhold,
895 New York.
- 896 Long, A.J., Woodroffe, S.A., Roberts, D.H., Dawson, S., 2011. Isolation basins, sea-level changes and the
897 Holocene history of the Greenland Ice Sheet. *Quat. Sci. Rev.* 30, 3748–3768.
898 <https://doi.org/10.1016/j.quascirev.2011.10.013>
- 899 Magaš, N., 1968. Osnovna geološka karta SFRJ, list Cres, 1:100 000, L33-113 (Basic Geological Map of
900 SFRJ: Cres Sheet L33-113). Institut za geološka istraživanja, Zagreb. Savezni geološki zavod,
901 Beograd.
- 902 Major, C., Ryan, W., Lericolais, G., Hajdas, I., 2002. Constraints on Black Sea outflow to the Sea of
903 Marmara during the last glacial–interglacial transition. *Mar. Geol.* 190(1), 19–34.

904 Malez, M., Slepčević, A., Srdoč, D., 1979. Određivanje starosti metodom radioaktivnog ugljika
905 kvartarnim naslagama na nekim lokalitetima u Dinarskom kršu, Rad JAZU, 383, Razred za
906 prirodne znanosti 18, 227-271.

907 Mamužić, P., 1968. Osnovna geološka karta SFRJ, list Lošinj, 1:100 000, L33-125 (Basic Geological Map
908 of SFRJ: Cres Sheet L33-125). Institut za geološka istraživanja, Zagreb. Savezni geološki zavod,
909 Beograd.

910 Marriner, N., Morhange, C., Faivre, S., Flaux, C., Vacchi, M., Miko, S., Dumas, V., Boetto, G., Radić Rossi,
911 I., 2014. Post-Roman sea-level changes on Pag Island (Adriatic Sea): Dating Croatia's
912 "enigmatic" coastal notch? *Geomorphology* 221, 83–94.
913 <https://doi.org/10.1016/j.geomorph.2014.06.002>

914 Maselli, V., Hutton, E.W., Kettner, A.J., Syvitski, J.P.M., Trincardi, F., 2011. High-frequency sea level and
915 sediment supply fluctuations during Termination I: An integrated sequence-stratigraphy and
916 modeling approach from the Adriatic Sea (Central Mediterranean). *Mar. Geol.* 287, 54–70.
917 <https://doi.org/10.1016/j.margeo.2011.06.012>

918 Maselli, V., Trincardi, F., 2013. Large-scale single incised valley from a small catchment basin on the
919 western Adriatic margin (central Mediterranean Sea). *Glob. Planet. Change* 100, 245–262.
920 <https://doi.org/10.1016/j.gloplacha.2012.10.008>

921 Meyers, P.A., 1994. Preservation of elemental and isotopic source identification of sedimentary
922 organic matter. *Chem. Geol.* 114, 289–302. [https://doi.org/10.1016/0009-2541\(94\)90059-0](https://doi.org/10.1016/0009-2541(94)90059-0)

923 Meyers, P.A., 2003. Application of organic geochemistry to paleolimnological reconstruction: a
924 summary of examples from the Laurentian Great Lakes. *Org. Geochem.* 34, 261–289.
925 [https://doi.org/10.1016/S0146-6380\(02\)00168-7](https://doi.org/10.1016/S0146-6380(02)00168-7)

926 Micallef, A., Foglini, F., Le Bas, T., Angeletti, L., Maselli, V., Pasuto, A., Taviani, M., 2013. The submerged
927 paleolandscape of the maltese Islands: Morphology, evolution and relation to quaternary
928 environmental change. *Mar. Geol.* 335, 129–147.
929 <https://doi.org/10.1016/j.margeo.2012.10.017>

930 Miko, S., Ilijanić, N., Hasan, O., Razum, I., Durn, T., Brunović, D., Papatheodorou, G., Bakrač, K., Hajek-
931 Tadesse, V., Crmarić, R., 2016. Late Quaternary evolution of lakes and submerged paleo-karst
932 on the Eastern Adriatic. Lake-Basin evolution, RCMNS Interim Colloquium 2016, Croatian
933 Geological Society Limnogeology, Zagreb, 2016.

934 Mikulčić Pavlaković, S., Crnjaković, M., Tibljaš, D., Šoufek, M., Wacha, L., Frechen, M., Lacković, D.,
935 2011. Mineralogical and geochemical characteristics of Quaternary sediments from the Island
936 of Susak (Northern Adriatic, Croatia). *Quat. Int.* 234, 32–49.
937 <https://doi.org/10.1016/j.quaint.2010.02.005>

938 Mitchum, R. M., Jr, Vail, P. R., Sangree, J. B., 1977. Seismic stratigraphy and global changes of sea level:
939 Part 6. Stratigraphic interpretation of seismic reflection patterns in depositional sequences, in:
940 Payton, C.E. (Eds.), *Seismic Stratigraphy - Applications to Hydrocarbon Exploration*, Am. Assoc.
941 *Pet. Geol. Bull.* 26, pp. 53-62. <https://doi.org/10.1306/M26490>

942 Mocochain, L., Clauzon, G., Bigot, J.Y., Brunet, P., 2006. Geodynamic evolution of the peri-
943 Mediterranean karst during the Messinian and the Pliocene: evidence from the Ardèche and
944 Rhône Valley systems canyons, Southern France. *Sediment. Geol.* 188–189, 219–233.
945 <https://doi.org/10.1016/j.sedgeo.2006.03.006>

946 Moscon, G., Correggiari, A., Stefani, C., Moscon, G., Correggiari, A., Stefani, C., Fontana, A., Remia, A.,
947 2015. Very-high resolution analysis of a transgressive deposit in the Northern Adriatic Sea
948 (Italy). *Alp. Mediterr. Quat.* 28, 121–129.

949 Murray, J.W., 2006. Ecology and Applications of Benthic Foraminifera. Cambridge University Press,
950 Cambridge.

951 Murray, J.W., Whittaker, J.E., Alve, E., 2000. On the type species of *Aubignyna* and a description of *A.*
952 *hamblensis*, a new microforaminifer from temperate shallow waters. *J. Micropalaeontology*
953 19, 61–67. <https://doi.org/10.1144/jm.19.1.61>

954 Murray, M., 2002. Is laser particle size determination possible for carbonate rich lake sediments? *J.*
955 *Paleolimnol.* 27, 173–183.

956 Narančić, B., Pienitz, R., Chaplignin, B., Meyer, H., Francus, P., Guilbault, J. P., 2016. Postglacial
957 environmental succession of Nettilling Lake (Baffin Island, Canadian Arctic) inferred from
958 biogeochemical and microfossil proxies. *Quaternary Science Reviews* 147, 391–405.
959 <https://doi.org/10.1016/j.quascirev.2015.12.022>

960 Normandeau, A., Lajeunesse, P., Trottier, A.-P., Poiré, A. G., Pienitz, R., 2017. Sedimentation in isolated
961 glaciomarine embayments during glacio-isostatically induced relative sea level fall (northern
962 Champlain Sea basin). *Canadian Journal of Earth Sciences* 54, 1049-1062.
963 <https://doi.org/10.1139/cjes-2017-0002>

964 Paskoff, R.P., 2005. Karst coasts, in: Schwartz, M. (Eds.), *Encyclopedia of Coastal Science*. *Encyclopedia*
965 *of Earth Sciences Series*. Dordrecht, The Netherlands: Springer, pp. 581–586.

966 Pellegrini, C., Asioli, A., Bohacs, K.M., Drexler, T.M., Feldman, H.R., Sweet, M.L., Maselli, V., Rovere, M.,
967 Gamberi, F., Valle, G.D., Trincardi, F., 2018. The late Pleistocene Po River lowstand wedge in
968 the Adriatic Sea: Controls on architecture variability and sediment partitioning. *Mar. Pet. Geol.*
969 96, 16–50. <https://doi.org/10.1016/j.marpetgeo.2018.03.002>

970 Pikelj, K., Juračić, M., 2013. Eastern Adriatic Coast (EAC): Geomorphology and Coastal Vulnerability of
971 a Karstic Coast. *J. Coast. Res.* 289, 944–957. <https://doi.org/10.2112/JCOASTRES-D-12-00136.1>

972 Piva, A., Asioli, A., Schneider, R.R., Trincardi, F., Andersen, N., Colmenero-Hidalgo, E., Dennielou, B.,
973 Flores, J.A., Vigliotti, L., 2008. Climatic cycles as expressed in sediments of the PROMESSI
974 borehole PRAD1-2, central Adriatic, for the last 370 ka: 1. Integrated stratigraphy.
975 *Geochemistry, Geophys. Geosystems* 9. <https://doi.org/10.1029/2007GC001713>

976 Rasmussen, S.O., Bigler, M., Blockley, S.P., Blunier, T., Buchardt, S.L., Clausen, H.B., Cvijanovic, I., Dahl-
977 Jensen, D., Johnsen, S.J., Fischer, H., Gkinis, V., Guillevic, M., Hoek, W.Z., Lowe, J.J., Pedro, J.B.,
978 Popp, T., Seierstad, I.K., Steffensen, J.P., Svensson, A.M., Vallelonga, P., Vinther, B.M., Walker,
979 M.J.C., Wheatley, J.J., Winstrup, M., 2014. A stratigraphic framework for abrupt climatic
980 changes during the Last Glacial period based on three synchronized Greenland ice-core
981 records: Refining and extending the INTIMATE event stratigraphy. *Quat. Sci. Rev.* 106, 14–28.
982 <https://doi.org/10.1016/j.quascirev.2014.09.007>

983 Reimer, P.J., Bard, E., Bayliss, A., Beck, J.W., Blackwell, P.G., Ramsey, C.B., Buck, C.E., Cheng, H.,
984 Edwards, R.L., Friedrich, M., Grootes, P.M., Guilderson, T.P., Haflidason, H., Hajdas, I., Hatté,
985 C., Heaton, T.J., Hoffmann, D.L., Hogg, A.G., Hughen, K.A., Kaiser, K.F., Kromer, B., Manning,
986 S.W., Niu, M., Reimer, R.W., Richards, D.A., Scott, E.M., Southon, J.R., Staff, R.A., Turney,
987 C.S.M., van der Plicht, J., 2013. IntCal13 and Marine13 Radiocarbon Age Calibration Curves 0–
988 50,000 Years cal BP. *Radiocarbon* 55, 1869–1887. https://doi.org/10.2458/azu_js_rc.55.16947

989 Ridente, D., Trincardi, F., Piva, A., Asioli, A., Cattaneo, A., 2008. Sedimentary response to climate and
990 sea level changes during the past 400 ka from borehole PRAD1-2 (Adriatic margin).
991 *Geochemistry, Geophys. Geosystems* 9, 1–20. <https://doi.org/10.1029/2007GC001783>

992 Rohling, E.J., Grant, K., Hemleben, C., Kucera, M., Roberts, A.P., Schmeltzer, I., Schulz, H., Siccha, M.,
993 Siddall, M., Trommer, G., 2008. New constraints on the timing of sea level fluctuations during
994 early to middle marine isotope stage 3. *Paleoceanography* 23.
995 <https://doi.org/10.1029/2008PA001617>

- 996 Rohling, E.J., Foster, G.L., Grant, K.M., Marino, G., Roberts, A.P., Tamisiea, M.E., Williams, F., 2014. Sea-
997 level and deep-sea-temperature variability over the past 5.3 million years. *Nature* 508, 477–
998 482. <https://doi.org/10.1038/nature13230>
- 999 Ronchi, L., Fontana, A., Correggiari, A., Asioli, A., 2018. Late Quaternary incised and infilled landforms
1000 in the shelf of the northern Adriatic Sea (Italy). *Mar. Geol.* 405, 47–67.
1001 <https://doi.org/10.1016/j.margeo.2018.08.004>
- 1002 Rovere, A., Stocchi, P., Vacchi, M., 2016. Eustatic and Relative Sea Level Changes. *Current Climate*
1003 *Change Reports* 2(4), 221–231. <https://doi.org/10.1007/s40641-016-0045-7>
- 1004 Roveri, M., Flecker, R., Krijgsman, W., Lofi, J., Lugli, S., Manzi, V., Sierro, F.J., Bertini, A., Camerlenghi,
1005 A., De Lange, G., Govers, R., Hilgen, F.J., Hübscher, C., Meijer, P.T., Stoica, M., 2014. The
1006 Messinian Salinity Crisis: Past and future of a great challenge for marine sciences. *Mar. Geol.*
1007 352, 25–58. <https://doi.org/10.1016/j.margeo.2014.02.002>
- 1008 Schmidt, R., Müller, J., Drescher-Schneider, R., Krisai, R., Szeroczyńska, K., Barić, A., 2000. Changes in
1009 lake level and trophy at Lake Vrana, a large karstic lake on the Island of Cres (Croatia), with
1010 respect to palaeoclimate and anthropogenic impacts during the last approx. 16,000 years. *J.*
1011 *Limnol.* 59, 113–130. <https://doi.org/10.4081/jlimnol.2000.113>
- 1012 Schmidt, R., Pugliese, N., Müller, J., Szeroczyńska, K., Bogner, D., Melis, R., Kamenik, C., Bari, A.,
1013 Danielopol, D.L., 2001. Palaeoclimate, vegetation and coastal lake development, from the
1014 Pleniglacial until early Holocene, in the northern Adriatic Valun bay (Isle of Cres, Croatia). *Quat.*
1015 *J Quat Sci* 14, 61–78.
- 1016 Seddon, M.B., Killeen, I.J., Fowles, A.P., 2014. A review of the non-marine Mollusca of Great Britain:
1017 Species status No. 17. *NRW Evid. Rep. No.14* 84.

- 1018 Shackleton, N.J. (1987): Oxygen isotopes, ice volume and sea level. *Quat. Sci. Rev.* 6, 183–190.
1019 [https://doi.org/10.1016/0277-3791\(87\)90003-5](https://doi.org/10.1016/0277-3791(87)90003-5)
- 1020 Shaw, T.A., Kirby, J.R., Holgate, S., Tutman, P., Plater, A.J., 2016. Contemporary Salt-Marsh
1021 Foraminiferal Distribution From the Adriatic Coast of Croatia and Its Potential for Sea-Level
1022 Studies. *J. Foraminifer. Res.* 46, 314–332. <https://doi.org/10.2113/gsjfr.46.3.314>
- 1023 Shaw, T. A., Plater, A. J., Kirby, J. R., Roy, K., Holgate, S., Tutman, P., Cahill, N., Horton, B. P., 2018.
1024 Tectonic influences on late Holocene relative sea levels from the central-eastern Adriatic coast
1025 of Croatia. *Quaternary Science Reviews* 200, 262–275.
1026 <https://doi.org/10.1016/j.quascirev.2018.09.015>
- 1027 Shinn, E., Reich, C., Locker, S., Hine, A., 1996. A giant sediment trap in the Florida Keys. *J. Coast. Res.*
1028 12, 953–959.
- 1029 Siddall, M., Rohling, E., Almogi-Labin, a, Hemleben, C., Meischner, D., Schmelzer, I., Smeed, D. A., 2003.
1030 Sea-level fluctuations during the last glacial cycle. *Nature* 423, 853–858.
1031 <https://doi.org/10.1038/nature01687.1>.
- 1032 Siddall, M., Rohling, E.J., Thompson, W.G., Waelbroeck, C., 2008. Marine Isotope Stage 3 sea level
1033 fluctuations: data synthesis and new outlook. *Rev. Geophys.* 46, 1–29.
1034 <https://doi.org/10.1029/2007RG000226.1>.
- 1035 Sivan, D., Wdowinski, S., Lambeck, K., Galili, E., Raban, A., 2001. Holocene sea-level changes along the
1036 Mediterranean coast of Israel, based on archaeological observations and numerical model.
1037 *Palaeogeography, Palaeoclimatology, Palaeoecology* 167(1–2), 101–117.
1038 [https://doi.org/10.1016/S0031-0182\(00\)00234-0](https://doi.org/10.1016/S0031-0182(00)00234-0)
- 1039 Stuiver M., Polach, H.A., 1977. Discussion: reporting of ^{14}C data. *Radiocarbon* 19(3), 355–63.

- 1040 Surić, M., 2002. Submarine Karst of Croatia - Evidence of Former Lower Sea Levels, Podmorski Kras Na
1041 Hrvaškem - Dokaz O Nekdanji Nižji Morski Gladini. *Acta Carsologica* 31, 89–98.
- 1042 Surić, M., 2005. Submerged karst – dead or alive? Examples from the Eastern Adriatic Coast (Croatia).
1043 *Geoadria* 10/1, 5-19.
- 1044 Surić, M., Juračić, M., 2010. Late Pleistocene-Holocene environmental changes – records from
1045 submerged speleothems along the Eastern Adriatic coast (Croatia). *Geol. Croat.* 63, 155–169.
1046 <https://doi.org/10.4154/gc.2010.13>
- 1047 Surić, M., Juračić, M., Horvatinčić, N., Krajcar Bronić, I., 2005. Late Pleistocene-Holocene sea-level rise
1048 and the pattern of coastal karst inundation: Records from submerged speleothems along the
1049 Eastern Adriatic Coast (Croatia). *Mar. Geol.* 214, 163–175.
1050 <https://doi.org/10.1016/j.margeo.2004.10.030>
- 1051 Surić, M., Korbar, T., Juračić, M., 2014. Tectonic constraints on the late Pleistocene-Holocene relative
1052 sea-level change along the north-eastern Adriatic coast (Croatia). *Geomorphology* 220, 93–
1053 103. <https://doi.org/10.1016/j.geomorph.2014.06.001>
- 1054 Surić, M., Richards, D.A., Hoffmann, D.L., Tibljaš, D., Juračić, M., 2009. Sea-level change during MIS 5a
1055 based on submerged speleothems from the eastern Adriatic Sea (Croatia). *Mar. Geol.* 262, 62–
1056 67. <https://doi.org/10.1016/j.margeo.2009.03.005>
- 1057 Taviani, M., Angeletti, L., Çağatay, M.N., Gasperini, L., Polonia, A., Wesselingh, F.P., 2014. Sedimentary
1058 and faunal signatures of the post-glacial marine drowning of the Pontocaspian Gemlik “lake”
1059 (Sea of Marmara). *Quat. Int.* 345, 11–17. <https://doi.org/10.1016/j.quaint.2014.05.045>
- 1060 Trobec, A., Šmuc, A., Poglajen, S., Vrabec, M., 2017. Submerged and buried Pleistocene river channels
1061 in the Gulf of Trieste (Northern Adriatic Sea): Geomorphic, stratigraphic and tectonic
1062 inferences. *Geomorphology* 286, 110-120. <https://doi.org/10.1016/j.geomorph.2017.03.012>

- 1063 Tung, J.W.T., Tanner, P.A., 2003. Instrumental determination of organic carbon in marine sediments.
1064 Mar. Chem. 80, 161–170. [https://doi.org/10.1016/S0304-4203\(02\)00116-0](https://doi.org/10.1016/S0304-4203(02)00116-0)
- 1065 Vacchi, M., Rovere, A., Chatzipetros, A., Zouros, N., Firpo, M., 2014. An updated database of Holocene
1066 relative sea level changes in NE Aegean Sea. Quat. Int. 328–329, 301–310.
1067 <https://doi.org/10.1016/j.quaint.2013.08.036>
- 1068 Vacchi, M., Marriner, N., Morhange, C., Spada, G., Fontana, A., Rovere, A., 2016. Multiproxy
1069 assessment of Holocene relative sea-level changes in the western Mediterranean: Sea-level
1070 variability and improvements in the definition of the isostatic signal. Earth-Science Rev. 155,
1071 172–197. <https://doi.org/10.1016/j.earscirev.2016.02.002>
- 1072 Valero-Garcés, B., Morellón, M., Moreno, A., Corella, J.P., Martín-Puertas, C., Barreiro, F., Pérez, A.,
1073 Giralt, S., Mata-Campo, M.P., 2014. Lacustrine carbonates of Iberian Karst Lakes: Sources,
1074 processes and depositional environments. Sediment. Geol. 299, 1–29.
1075 <https://doi.org/10.1016/j.sedgeo.2013.10.007>
- 1076 van Hengstum, P.J., Scott, D.B., 2011. Ecology of Foraminifera and Habitat Variability in an Underwater
1077 Cave: Distinguishing Anchialine Versus Submarine Cave Environments. J. Foraminifer. Res. 41,
1078 201–229. <https://doi.org/10.2113/gsjfr.41.3.201>
- 1079 van Hengstum, P.J., Scott, D.B., Gröcke, D.R., Charette, M.A., 2011. Sea level controls sedimentation
1080 and environments in coastal caves and sinkholes. Mar. Geol. 286, 35–50.
1081 <https://doi.org/10.1016/j.margeo.2011.05.004>
- 1082 Vidović, J., 2010. Analiza utjecaja prirodnih promjena i antropogenog djelovanja na zajednice
1083 foraminifera u sedimentima istočne obale Jadranskog mora. Unpubl. PhD Thesis, Faculty of
1084 Science, University of Zagreb.

- 1085 Vlahović, I., Tišljarić, J., Velić, I., Matičec, D., 2005. Evolution of the Adriatic Carbonate Platform:
1086 Palaeogeography, main events and depositional dynamics. *Palaeogeogr. Palaeoclimatol.*
1087 *Palaeoecol.* 220, 333–360. <https://doi.org/10.1016/j.palaeo.2005.01.011>
- 1088 Wacha, L., Mikulčić Pavlaković, S., Novothny, Á., Crnjaković, M., Frechen, M., 2011a. Luminescence
1089 dating of Upper Pleistocene loess from the Island of Susak in Croatia. *Quat. Int.* 234, 50-61.
- 1090 Wacha, L., Mikulčić Pavlaković, S., Frechen, M., Crnjaković, M., 2011b. The Loess chronology of the
1091 Island of Susak, Croatia. *EandG - Q. Sci. J.* 60, 153–169.
- 1092 Wacha, L., Rolf, C., Hambach, U., Frechen, M., Galović, L., Duchoslav, M., 2017. The Last Glacial aeolian
1093 record of the Island of Susak (Croatia) as seen from a high-resolution grain-size and rock
1094 magnetic analysis. *Quat. Int.* 1–14. <https://doi.org/10.1016/j.quaint.2017.08.016>
- 1095 Waelbroeck, C., Labeyrie, L., Michel, E., Duplessy, J.C., McManus, J.F., Lambeck, K., Balbon, E.,
1096 Labracherie, M., 2002. Sea-level and deep water temperature changes derived from benthic
1097 foraminifera isotopic records. *Quat. Sci. Rev.* 21, 295–305. [https://doi.org/10.1016/S0277-](https://doi.org/10.1016/S0277-3791(01)00101-9)
1098 [3791\(01\)00101-9](https://doi.org/10.1016/S0277-3791(01)00101-9)
- 1099 Wahl, T., Haigh, I.D., Nicholls, R.J., Arns, A., Dangendorf, S., Hinkel, J., Slangen, A.B.A., 2017.
1100 Understanding extreme sea levels for broad-scale coastal impact and adaptation analysis. *Nat.*
1101 *Commun.* 8, 1–12. <https://doi.org/10.1038/ncomms16075>
- 1102 Wunsam, S., Schmidt, R., Müller, J., 1999. Holocene lake development of two dalmatian lagoons (Malo
1103 and Veliko Jezero, Isle of Mljet) in respect to changes in Adriatic sea level and climate.
1104 *Palaeogeogr. Palaeoclimatol. Palaeoecol.* 146, 251–281. [https://doi.org/10.1016/S0031-](https://doi.org/10.1016/S0031-0182(98)00147-3)
1105 [0182\(98\)00147-3](https://doi.org/10.1016/S0031-0182(98)00147-3)